CIRCULAR CYLINDRICAL DIELECTRIC-COATED METAL ROD EXCITED IN THE SYMMETRIC TM_{01} MODE

Part I. Surface-wave Propagation Characteristics

By T. CHANDRAKALADHARA RAO* AND R. CHATTERJEE

(Department of Electrical Communication Engineering, Indian Institute of Science, Bangalore-12, India)

Received June 25, 1973

ABSTRACT

The electromagnetic wave propogation characteristics of a circular cylindrical metal rod of finite conductivity coated with a lossy dielectric have been investigated. By applying the proper boundary conditions, the characteristic equation has been derived. This equation has been solved and the propagation characteristics like the phase constant, the attenuation constant, the phase velocity, the guide wavelength, the characteristic impedance, and the surface resistance have been determined and their variation with the different parameters have been studied in detail. The power carried by the surface wave and also the power handling capacity have been studied. Experimental work to verify some of the theoretical results have been reported.

1. INTRODUCTION

Investigations on the propagation of electromagnetic waves along a dielectric-coated metal wire were first initiated by Harms[1] in 1907. Later in 1950, Goubau[2] first demonstrated the physical reality of Sommerfeld's surface wave. His work[3-5] on a dielectric-coated conductor and a conductor with a modified surface was responsible for giving further insight into the characteristics of electromagnetic surface waves. After Goubau, several others have studied the different aspects of the surface waves. Barlow[6-8], Brown[9,10] Wait[11], Cullen[12,13], Zucker[14,15], Chatterjee[16,17] have contributed significantly to the understanding of surface wave propagation in general. Colin[18], Bercili[19], Semenov[20,21] and Kikuchi and Yamashita[22] have investigated the propagation over dielectric-coated metal wires in particular. It may be noted, however, that in the course of their investiga-

---

* At present with the Special Projects Team, Hindustan Aeronautics, Ltd., Hyderabad Division, Hyderabad-42.

tions. Goubau and other earlier investigators considered the metallic wire to be infinitely conducting and the dielectric layer to be thin and loss free. As far as is available from the published literature, it is found that there is very little information about the surface wave propagation on metal rods of finite conductivity with thick and lossy dielectric coatings. The object of this paper is to present the results of the investigations on the propagation characteristics of electromagnetic waves on a circular cylindrical dielectric-coated metal rod. The metal rod is of finite conductivity and the dielectric layer is thick and lossy.

2. GEOMETRY OF THE SYSTEM

The geometry of the system under investigation and the parameters of the different media are shown in Fig. 1. The wave is assumed to be

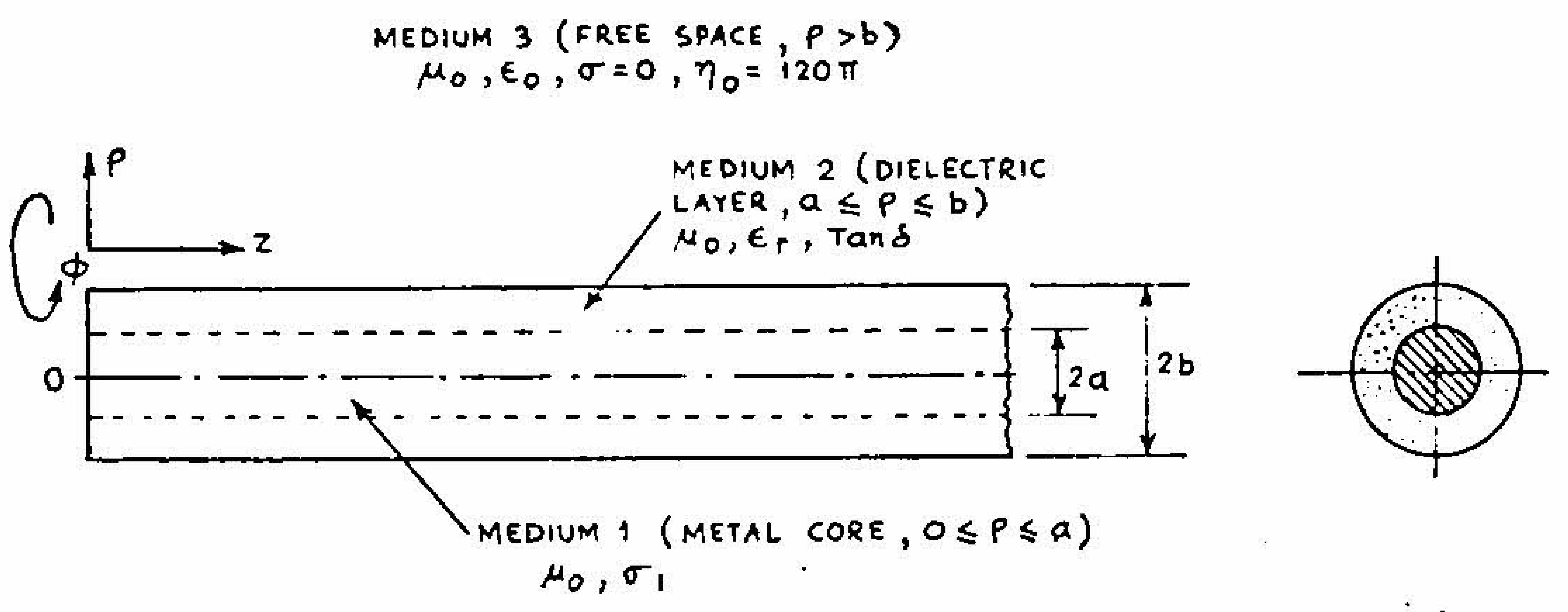

FIG. 1.

propagating in the positive Z-direction and the field components are assumed to vary as exp $(-\gamma z)$ where γ is the axial propagation constant. The propagation constant γ consists of a small real part 'α', the attenuation constant and a large imaginary part '$j\beta$' (β is real and is called the phase constant).

$$\gamma = \alpha + j\beta = j\beta\left\{1 - \frac{j\alpha}{\beta}\right\}. \tag{2.1}$$

A time variation of $\exp(j\omega t)$ is assumed.

Medium 3 ($\rho > b$, Free space) is characterized by its permeability μ_0, permittivity ϵ_0, intrinsic impedance $\eta_0 = \sqrt{\mu_0/\epsilon_0}$ and wave number $k_0 = \omega\sqrt{\mu_0/\epsilon_0}$. Medium 2 ($a \leqslant \rho \leqslant b$), the dielectric layer is represented by its permeability and permittivity normalized with the corresponding ones of medium 3.

$$\bar{\mu} = \frac{\mu_2}{\mu_0} = 1 \text{ (assuming } \mu_2 = \mu_0)$$

$$\bar{\epsilon} = \frac{\epsilon_2}{\epsilon_0} = \epsilon_r\,[1 - j\tan\delta] \tag{2.2}$$

where ϵ_r is the relative dielectric constant of the dielectric coating material and $\tan\delta$ is its loss tangent. The wave number k_2 in medium 2 is given by $k_2^2 = k_0^2\epsilon_r\,(1 - j\tan\delta)$. Medium 1 ($0 \leqslant \rho \leqslant a$, the metal core) is characterized by its permeability $\mu_1\,(= \mu_0)$ and conductivity σ_c.

$$k_0^2 = \omega^2\mu_0\epsilon_0.$$

3. Field Components

The field components of the TM_{01} mode obey circular symmetry and there is no variation of the field components with ϕ'. The three nonvanishing field components are E_z, E_ρ and $H_{\phi'}$. The wave equation $(\nabla^2 + \omega^2\mu\epsilon)\vec{E} = 0$ is solved for the E_z component. The solution of this equation is of the form

$$E_z = \begin{cases} [AJ_0(h\rho/b) + BY_0(h\rho/b)]\exp(-\gamma z) & \text{for } a \leqslant \rho \leqslant b \\ CK_0(g\rho/b)\exp(-\gamma z) & \text{for } \rho > b \end{cases} \tag{3.1}$$

where

$$h = b\sqrt{k_2^2 + \gamma^2}$$

and

$$g = jb\sqrt{k_0^2 + \gamma^2}. \tag{3.2}$$

$J_0(h\rho/b)$ = Bessel function, $Y_0(h\rho/b)$ = Nuemann function and $K_0(g\rho/b)$ = Modified Bessel function. The other two components can be determined from Maxwell's equations.

Hence, the field components are

$$\left.\begin{aligned} E_z &= [AJ_0(h\rho/b) + BY_0(h\rho/b)]\exp(-\gamma z) \\ H_{\phi'} &= \frac{-j\omega\epsilon_2 b}{h}[AJ_0'(h\rho/b) + BY_0'(h\rho/b)]\exp(-\gamma z) \\ E_\rho &= \frac{\gamma b}{h}[AJ_0'(h\rho/b) + BY_0'(h\rho/b)]\exp(-\gamma z) \end{aligned}\right\} \tag{3.3}$$

for $a \leqslant \rho \leqslant b$ in medium 2 and

$$\left.\begin{aligned} E_z &= CK_0(g\rho/b)\exp(-\gamma z) \\ H_\phi' &= \frac{j\omega\epsilon_0 b}{g} CK_0'(g\rho/b)\exp(-\gamma z) \\ E_\rho &= \frac{\gamma b}{g} CK_0'(g\rho/b)\exp(-\gamma z) \end{aligned}\right\} \tag{3.4}$$

for $\rho > b$, in medium 3.

4. CHARACTERISTIC EQUATION

By applying the following boundary conditions, the characteristic equation is obtained.

(i) $E_z = ZH_{\phi'}$ at the metal-dielectric boundary, $\rho = a$, where

$$Z = \sqrt{\frac{\omega\mu_0}{\sigma_c}} \angle 45^\circ = \text{surface impedance at the boundary.}$$

(ii) The two tangential field components E_z and H_ϕ' are matched at the dielectric-air boundary $\rho = b$.

From the boundary condition (i)

$$B = -A\frac{J_0(h/\sigma) - (1-j)\,GJ_0'(h/\sigma)}{Y_0(h/\sigma) - (1-j)\,GY_0'(h/\sigma)} \tag{4.1}$$

where

$$G = k_0^2\,\delta\,\epsilon_r b$$

$$\delta = \sqrt{\frac{2}{\omega\mu_0\sigma_c}} = \text{skindepth}$$

and

$$\sigma = b/a.$$

Matching E_z at $\rho = b$,

$$AJ_0(h) + BY_0(h) = CK_0(g)$$

or

$$A\left\{\frac{J_0(h)\,[Y_0(h/\sigma) - (1-j)\,GY_0'(h/\sigma)] - [J_0(h/\sigma) - (1-j)\,GJ_0'(h/\sigma)]\,Y_0'(h)}{Y_0(h/\sigma) - (1-j)\,Y_0'(h/\sigma)}\right\}$$
$$= CK_0(g). \tag{4.2}$$

Matching $H_{\phi'}$ at $\rho = b$.

$$-\frac{j\omega\epsilon_2 b}{h}\left[AJ_0'(h) + BY_0'(h)\right] = \frac{-j\omega\epsilon_0}{(-g)} bCK_0'(g) \tag{4.3}$$

or

$$\frac{\epsilon_r}{h} A \left\{\frac{J_0'(h)\left[Y_0\left(\frac{h}{\sigma}\right) - (1-j)\,GY_0'\left(\frac{h}{\sigma}\right)\right] - \left[J_0\left(\frac{h}{\sigma}\right) - (1-j)\,GJ_0'\left(\frac{h}{\sigma}\right)\right] Y_0'(h)}{Y_0\left(\frac{h}{\sigma}\right) - (1-j)\,GY_0'\left(\frac{h}{\sigma}\right)}\right\}$$

$$= -\frac{1}{g} CK_0'(g). \tag{4.4}$$

Dividing equation (4.4) by (4·2)

$$\frac{\epsilon_r}{h}\left\{\frac{\left[J_0'(h)\,Y_0\left(\frac{h}{\sigma}\right) - J_0\left(\frac{h}{\sigma}\right) Y_0'(h)\right] - (1-j)\,G\left[J_0'(h)\,Y_0'\left(\frac{h}{\sigma}\right) - J_0'\left(\frac{h}{\sigma}\right) Y_0'(h)\right]}{\left[J_0(h)\,Y_0\left(\frac{h}{\sigma}\right) - J_0\left(\frac{h}{\sigma}\right) Y_0(h)\right] - (1-j)\,G\left[J_0(h)\,Y_0'\left(\frac{h}{\sigma}\right) - J_0'\left(\frac{h}{\sigma}\right) Y_0(h)\right]}\right\}$$

$$= -\frac{1}{g}\frac{K_0'(g)}{K_0(g)}. \tag{4.5}$$

Let

$$P(h) = J_0(h)\,Y_0\left(\frac{h}{\sigma}\right) - J_0\left(\frac{h}{\sigma}\right) Y_0(h)$$

and

$$Q(h) = J_0(h)\,Y_0'\left(\frac{h}{\sigma}\right) - Y_0(h)\,J_0'\left(\frac{h}{\sigma}\right). \tag{4.6}$$

Keeping the (h/σ) term constant

$$P(h) = \frac{dP(h)}{dh}$$

$$= J_0'(h)\,Y_0\left(\frac{h}{\sigma}\right) - J_0\left(\frac{h}{\sigma}\right) Y_0'(h)$$

$$Q'(h) = J_0'(h)\,Y_0'\left(\frac{h}{\sigma}\right) - J_0'\left(\frac{h}{\sigma}\right) Y_0'(h).$$

The characteristic equation then simplifies to

$$\frac{\epsilon_r}{h}\frac{P(h) - (1-j)\,GQ'(h)}{P(h) - (1-j)\,GQ'(h)} = -\frac{1}{g}\frac{K_0'(g)}{K_0(g)}. \tag{4.7}$$

Let

$$\frac{1}{h}\frac{P'(h)}{P(h)} = f(h)$$

$$\frac{1}{(-g)}\frac{K_0'(g)}{K_0(g)} = \phi(g). \tag{4.8}$$

After some simplification, the characteristic equation is obtained in the form

$$\frac{1}{\phi(g)} = \frac{1}{\epsilon_T f(h)} + (1-j)\,\Delta R(h) \tag{4.9}$$

where

$$\Delta = 0\cdot 5bk_0^2\,\delta\sigma$$

and

$$R(h) = \frac{1}{\sigma}\left[\frac{P(h)\,Q'(h)}{P'^2(h)} - \frac{Q(h)}{P'(h)}\right]. \tag{4.10}$$

Equation (3.9) reduces to the form

$$\frac{1}{\phi(g)} = \frac{1}{\epsilon_T f(h)} \tag{4.11}$$

when the conductivity (σ_c) of the core metal is assumed to be infinite. Equation (4.11) is the characteristic equation using which the surface wave propagation characteristics have been studied by the earlier investigators.

The transverse propagation constants are related by

$$\frac{h^2}{b^2} - \left(\frac{-g^2}{b^2}\right) = k_2^2 - k_0^2$$

or

$$h^2 + g^2 = (k_2^2 - k_0^2). \tag{4.12}$$

Equations (4.10) and (4.12) are two equations in 'h' and 'g'. By separating the real and imaginary parts of the two equations, from the relations $h = h_1 - jh_2$ and $g = g_1 - jg_2$, four equations in h_1, h_2, g_1 and g_2 are obtained. While making the analysis, the second order terms like h_2/h_1, g_2/g_1, α/β, etc., are neglected in complarison with unity.

5. SOLUTION OF THE CHARACTERISTIC EQUATION

For $h_2 \ll h_1$ and $g_2 \ll g_1$, the functions $f(h)$ and $\phi(g)$ may be decomposed into their real and imaginary parts.

$$\left.\begin{aligned} f(h) &= f(h_1 - jh_2) = f(h_1) - jh_2 f'(h_1) \\ &\qquad\qquad\qquad\qquad \text{(using Taylors' series)} \\ &= f(h_1) + jh_1 h_2 N(h_1) \\ \phi(g) &= \phi(g_1 - jg_2) = \phi(g_1) - jg_2\phi'(g_1) \\ &= \phi(g_1) + jg_1 g_2 L(g_1) \end{aligned}\right\} \tag{5.1}$$

where

$$N(h_1) = -\frac{1}{h_1} f'(h_1)$$
$$= -f^2(h_1)[1 - R(h_1)] + \frac{1}{h_1^2}[1 + 2f(h_1)]$$

and

$$L(g_1) = -\frac{1}{g_1}\phi(g_1)$$
$$= -\phi^2(g_1) + \frac{1}{g_1^2}\{1 + 2\phi(g_1)\} \tag{5.2}$$

This decomposition is justified if the following inequality is satisfied.

$$\left(1 - \frac{1}{\epsilon_r}\right)(b - a) > 2\delta,$$

where

$$\delta = \text{skin depth}$$

Also

$$h = h_1\left[1 - \frac{jh_2}{h_1}\right] \simeq h_1$$

So

$$R(h) \approx R(h_1). \tag{5.3}$$

The complex characteristic equation simplifies to

$$\frac{1}{\epsilon_r\,[f(h_1) + jh_1h_2N(h_1)]} + (1 - j)\,\Delta\, R(h_1) = \frac{1}{\phi(g_1) + jg_1g_2L(g_1)}$$

or

$$\frac{1}{\epsilon_r f(h_1)}\left[1+\frac{jh_1h_2N(h_1)}{f(h_1)}\right]^{-1}+(1-j)\,\triangle\,R(h_1)$$

$$=\frac{1}{\phi(g_1)}\left[1+\frac{jg_1g_2L(g_1)}{\phi(g_1)}\right]^{-1} \tag{5.4}$$

Separating the real and imaginary parts

$$\frac{1}{\epsilon_r f(h_1)}+\triangle\,R(h_1)=\frac{1}{\phi(g_1)} \tag{5.5}$$

and

$$\frac{h_1h_2N(h_1)}{\epsilon_r f^2(h_1)}+\triangle\,R(h_1)=\frac{g_1g_2\,L(g_1)}{\phi^2(g_1)} \tag{5.6}$$

From equations (3.12)

$$\left.\begin{aligned}[h_1^2-jh_2]^2+[g_1-jg_2]^2&=(k_2^2-k_0^2)\,b^2\\ &=k_0^2b^2\,[\epsilon_r(1-j\tan\delta)-1]\\ h_1^2-2jh_1h_2+g_1^2-2jg_1g_2&=k_0^2\,b^2\,[\epsilon_r(1-j\tan\delta)-1]\end{aligned}\right\}. \tag{5.7}$$

Equating the real and imaginary parts

$$h_1^2+g_1^2=k_0^2b^2(\epsilon_r-1) \tag{5.8}$$

$$2\,[h_1h_2+g_1g_2]=k_0^2\,b^2\,\epsilon_r\tan\delta. \tag{5.9}$$

Equations (5.5) and (5.8) are solved for h_1 and g_1. Substituting these solutions in (5.6) and (5.9), h_2 and g_2 are found out.

Numerical calculations have been made for the following range of parameters:

(i) The ratio b/a is varied from 1·02 to 100 in discrete steps at a constant metal rod radius 'a' = 0·2 cm. The steps are as follows: 1·02, 1·25, 1·5, 2, 3, 4, 5, 6, 7, 8, 9, 10, 15, 20, 25, 30, 40, 50, 80, 100.

(ii) The conductor radius 'a' is varied from 1 mm to 1 cm in the following steps: 0·1, 0·2, 0·3, 0·5, 0·8, 1·0 cm.

(iii) The free-space wavelength 'λ_0' is varied from 0·5 cm to 10 cm in discrete steps: 0·5, 1, 2, 4, 8, 10 cm.

(iv) The dielectric constant ϵ_r is varied from a very low value to very high value. Only those dielectric materials are considered whose dielectric constants and loss tangents are known well at the operating frequency. Fig. 2 shows the variation of the radial propagation constant (real part

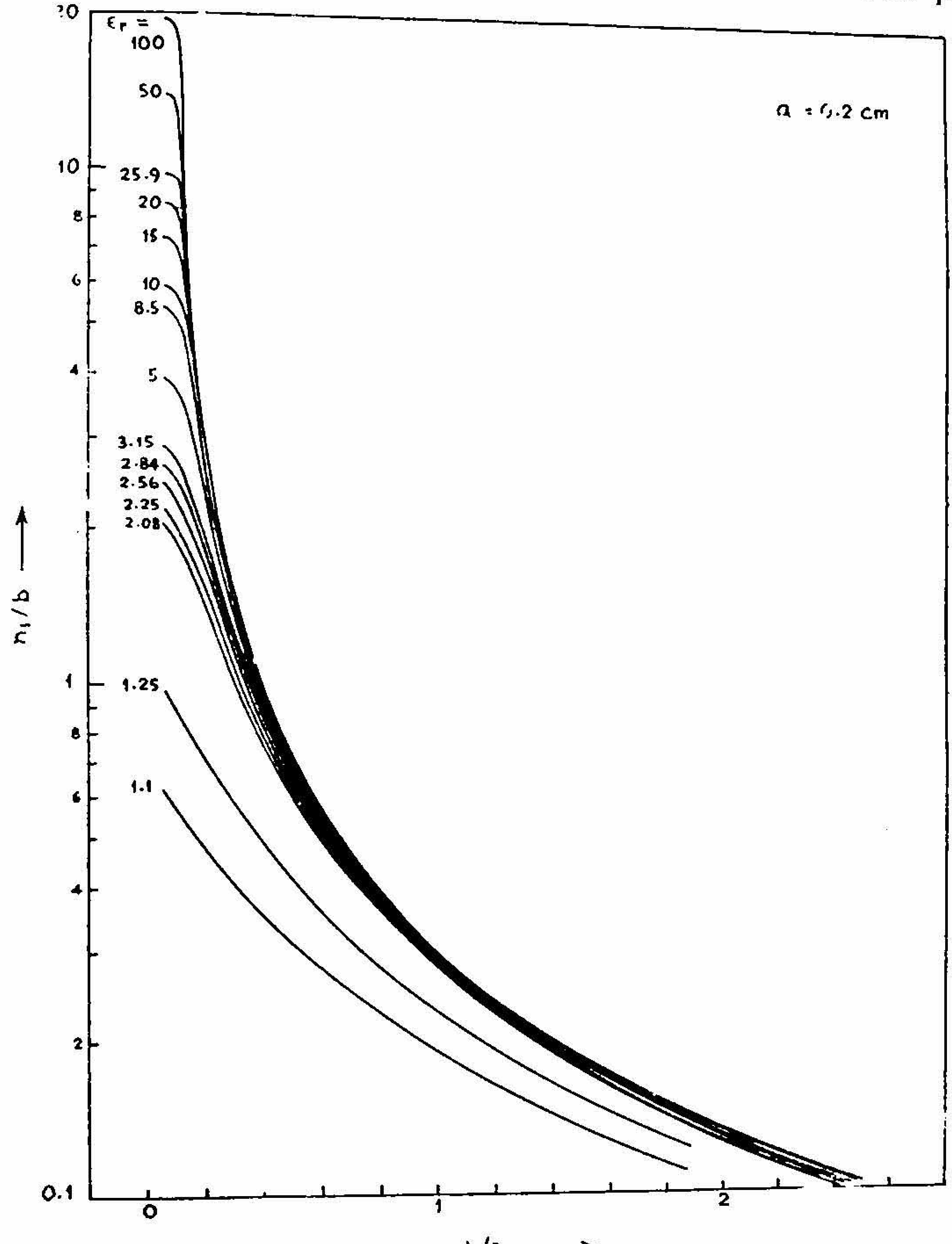

FIG. 2. Variation of the radial propagation constant inside the dielectric layer (real part h_1/b) with b/λ_0. $\lambda_0 = 3 \cdot 2$ cm.

h_1/b) inside the dielectric layer with b/λ_0, for $\lambda_0 = 3 \cdot 2$ cm. Fig. 3 shows the variation of the radial propagation constant inside the dielectric layer (real part h_1/b and imaginary part h_2/b) with frequency for $\epsilon_r = 2 \cdot 56$.

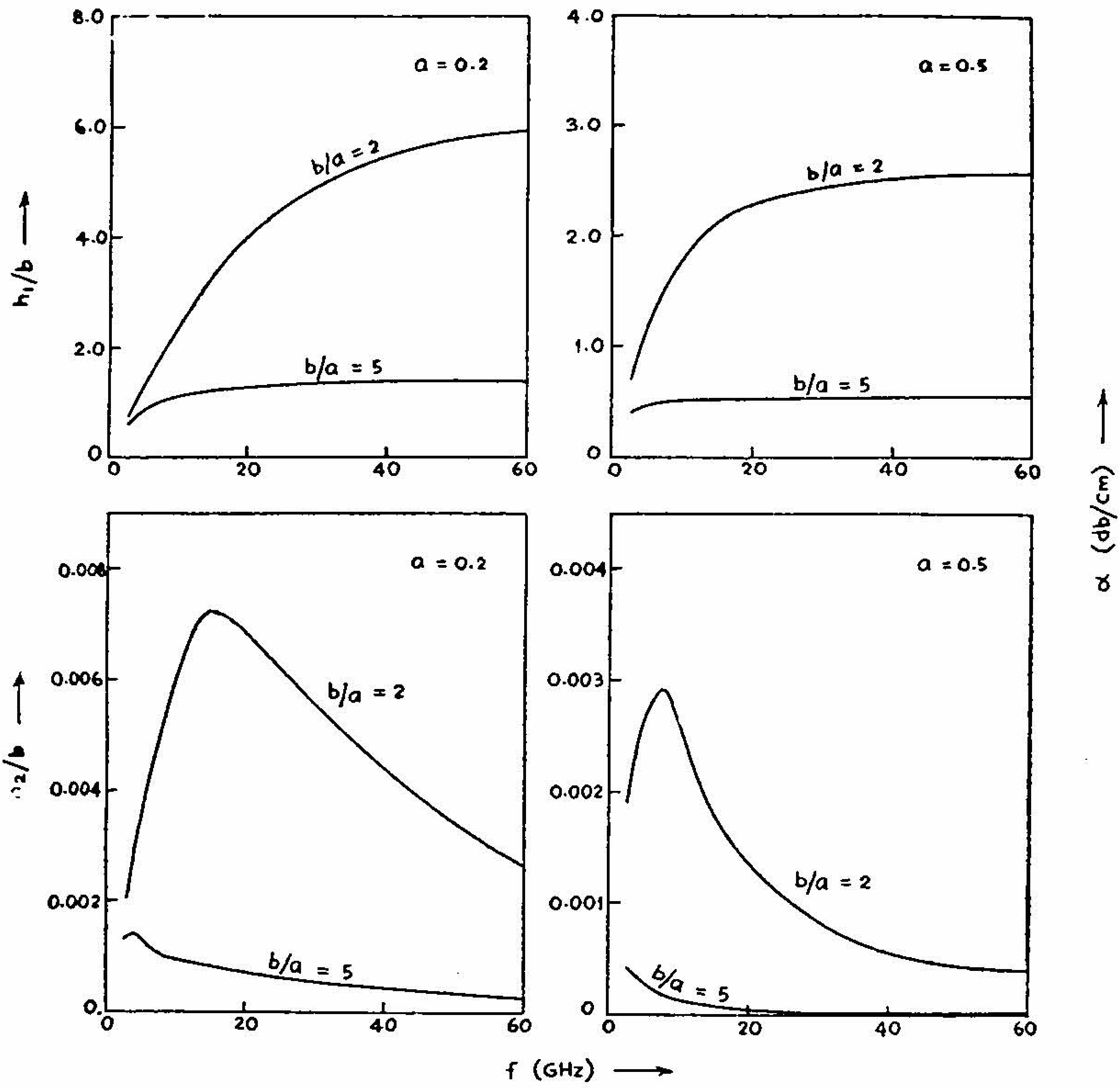

FIG. 3. Variation of the radial propagation constant inside the dielectric layer (real part h_1/b and imaginary part h_2/b) with frequency $\epsilon_r = 2 \cdot 56$.

Fig. 4 shows the variation of the radial propagation constant outside the dielectric layer (real part g_1/b) with b/λ_0, for $\lambda_0 = 3 \cdot 2$ cm.

Fig. 5 shows the variation of the radial propagation constant outside the dielectric layer (imaginary part g_2/b) with b/λ_0 at $\lambda_0 = 3 \cdot 2$ cm.

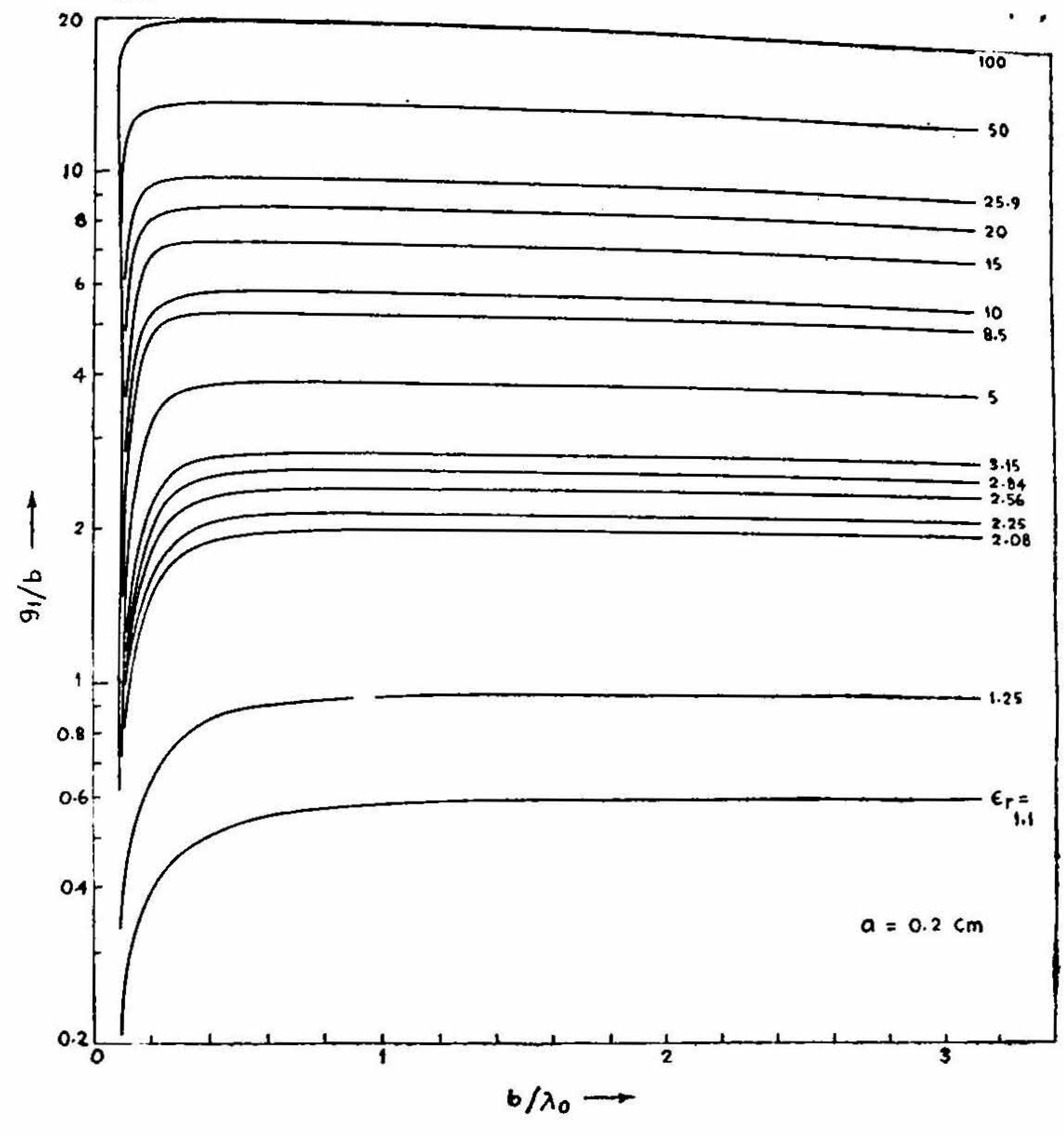

FIG. 4. Variation of the radial propagation constant outside the dielectric layer (real part g_1/b) with b/λ_0. $\lambda_0 = 3\cdot 2$ cm.

Fig. 6 shows the variation of the radial propagation constant outside the dielectric layer (real part g_1/b and imaginary part g_2/b) with frequency for $\epsilon_r = 2\cdot 56$.

6. Attenuation and Phase Constants

In medium 3 ($\rho > b$), the radial propagation constant is given by

$$-\frac{g^2}{b^2} = k_0^2 - p^2 = k_0^2 + \gamma^2$$

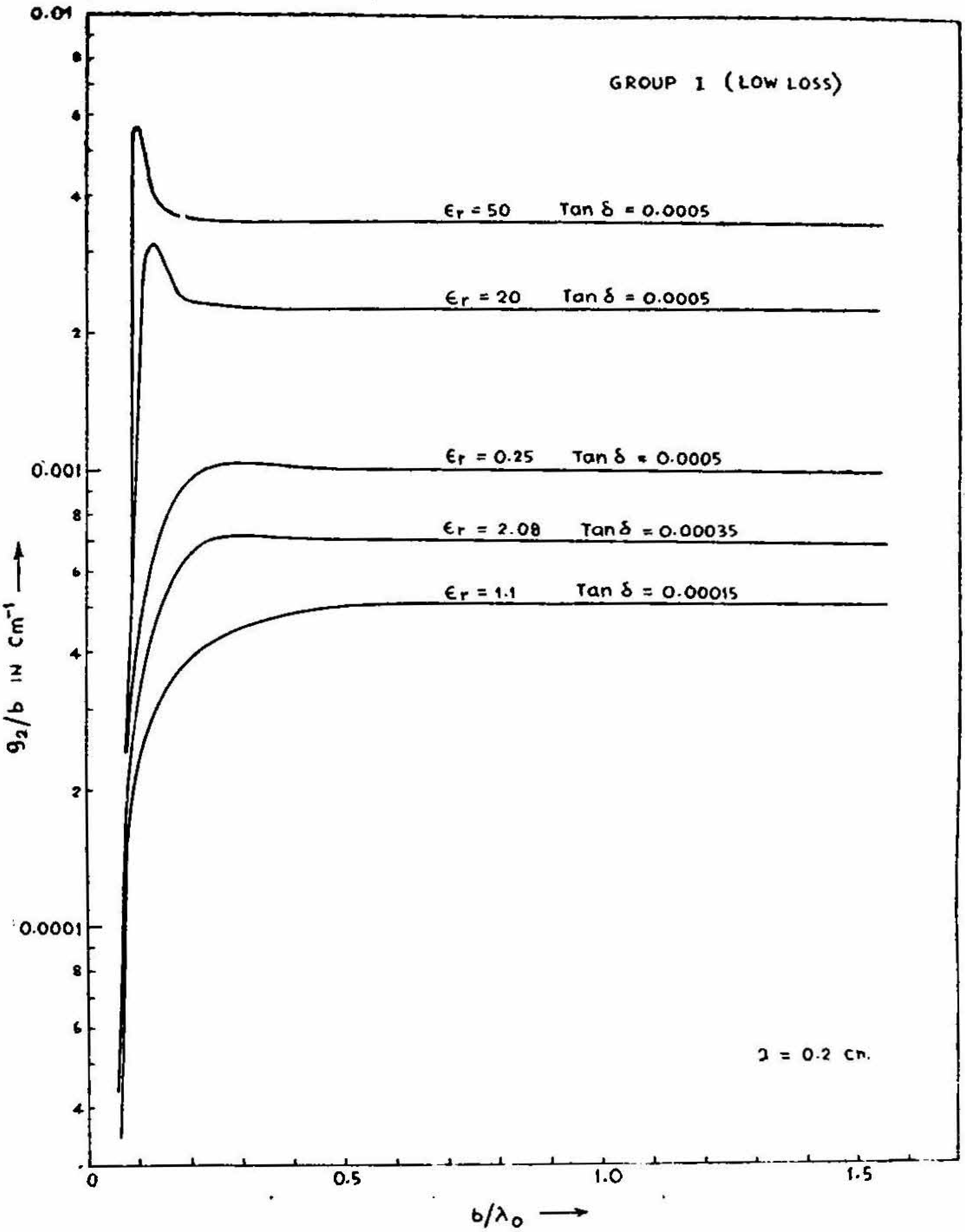

FIG. 5. Variation of the radial propagation constant outside the dielectric layer (imaginary part g_2/b) with b/λ_0. $\lambda_0 = 3\cdot 2$ cm.

or

$$p^2 = k_0^2 + \frac{g^2}{b^2}$$

$$[\beta - ja]^2 = k_0^2 + \frac{(g_1 - jg_2)^2}{b^2}$$

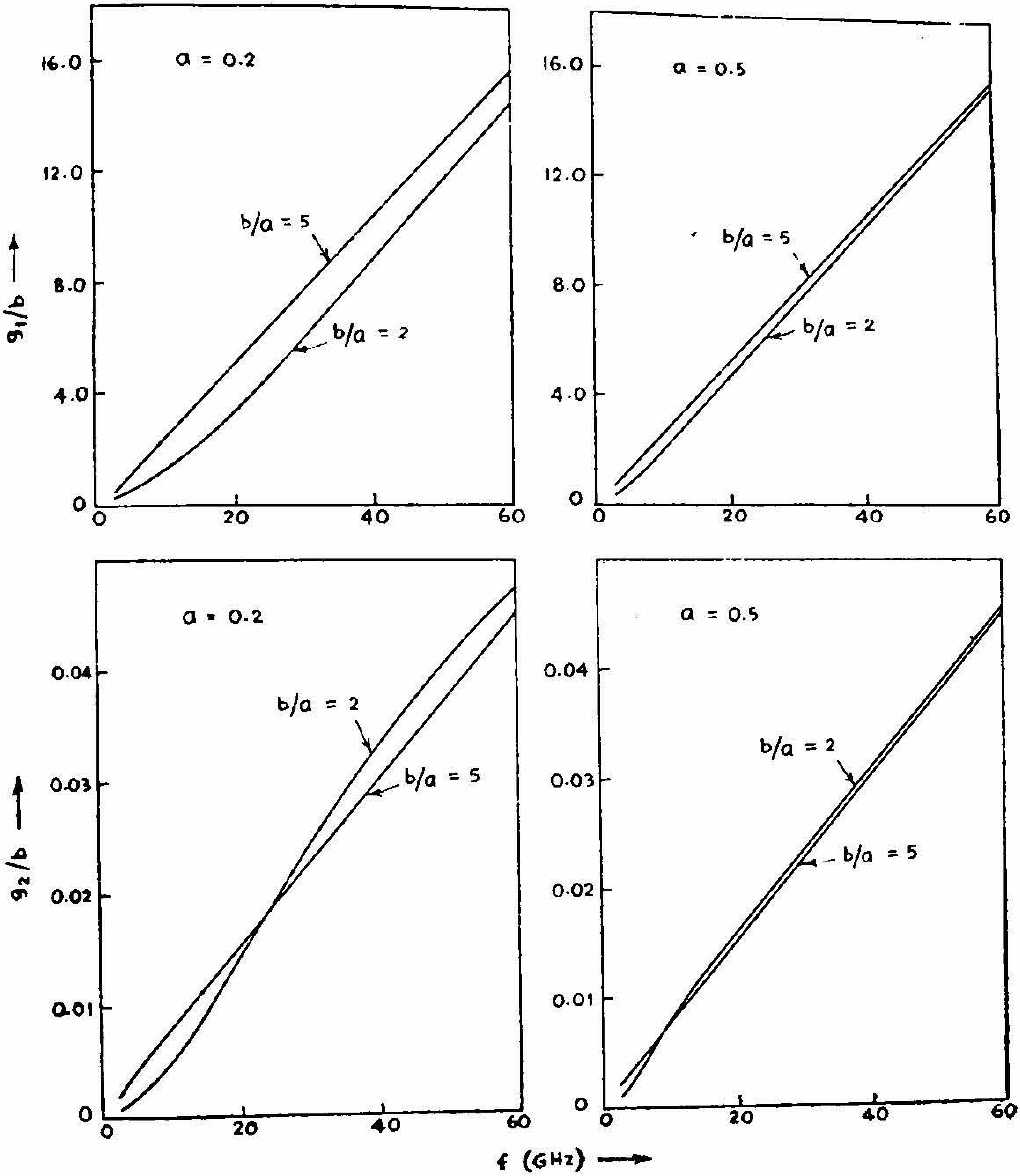

FIG. 6. Variation of the radial propagation constant outside the dielectric layer (real part g_1/b, imaginary part g_2/b) with frequency. $\epsilon_r = 2 \cdot 56$.

where

$$p = jr \tag{6.1}$$

$$\beta^2 \left[1 - \frac{j\alpha}{\beta}\right]^2 = k_0^2 + \frac{(g_1^2 - g_2^2) - 2jg_1g_2}{b^2}$$

$$\beta^2 - 2j\alpha\beta = \left[k_0^2 + \frac{g_1^2 - g_2^2}{b^2}\right] - \frac{2jg_1g_2}{b^2}. \tag{6.2}$$

Equating real and imaginary parts

$$\beta^2 = k_0^{\,2} + \frac{g_1^{\,2} - g_2^{\,2}}{b^2} \tag{6.3}$$

and

$$a\beta = \frac{g_1 g_2}{b^2}$$

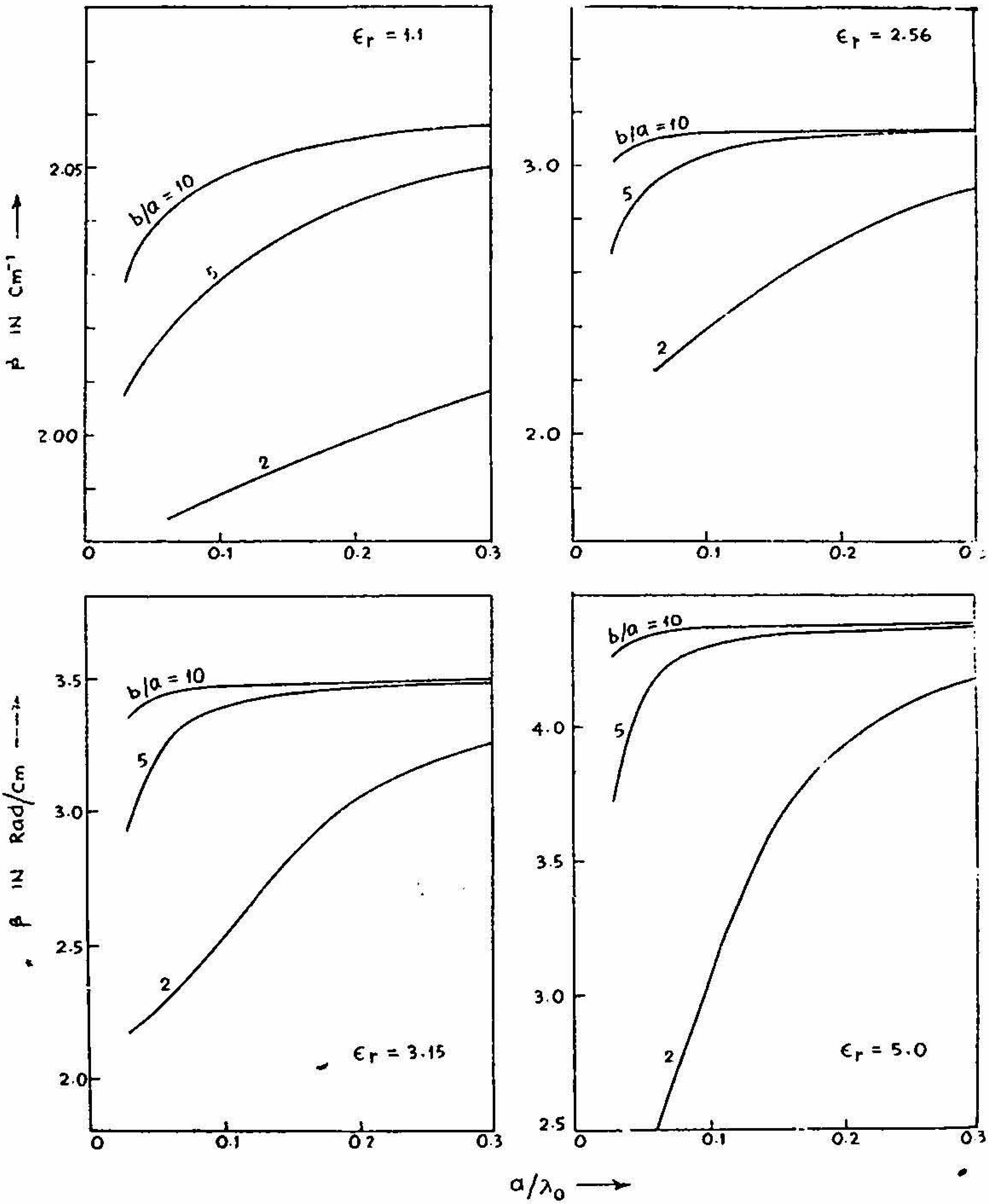

FIG. 7. Variation of the phase constant (β) with a/λ_0. $\lambda_0 = 3 \cdot 2$ cm.

Hence, the Phase Constant

$$\beta = \sqrt{k_0^2 + \frac{g_1^2 - g_2^2}{b^2}} \tag{6.4}$$

and the attenuation constant

$$\alpha = \frac{g_1 g_2}{b^2 \beta}. \tag{6.5}$$

Fig. 7 shows the variation of the phase constant β with a/λ_0 at $\lambda_0 = 3 \cdot 2$ cm.

Fig. 8 shows the variation of β with b/a ratio.

Figs. 9 (*a*) and (*b*) show the variation of the attenuation constant α with b/a.

Fig. 10 shows the variation of α with frequency for $\epsilon_r = 2 \cdot 56$.

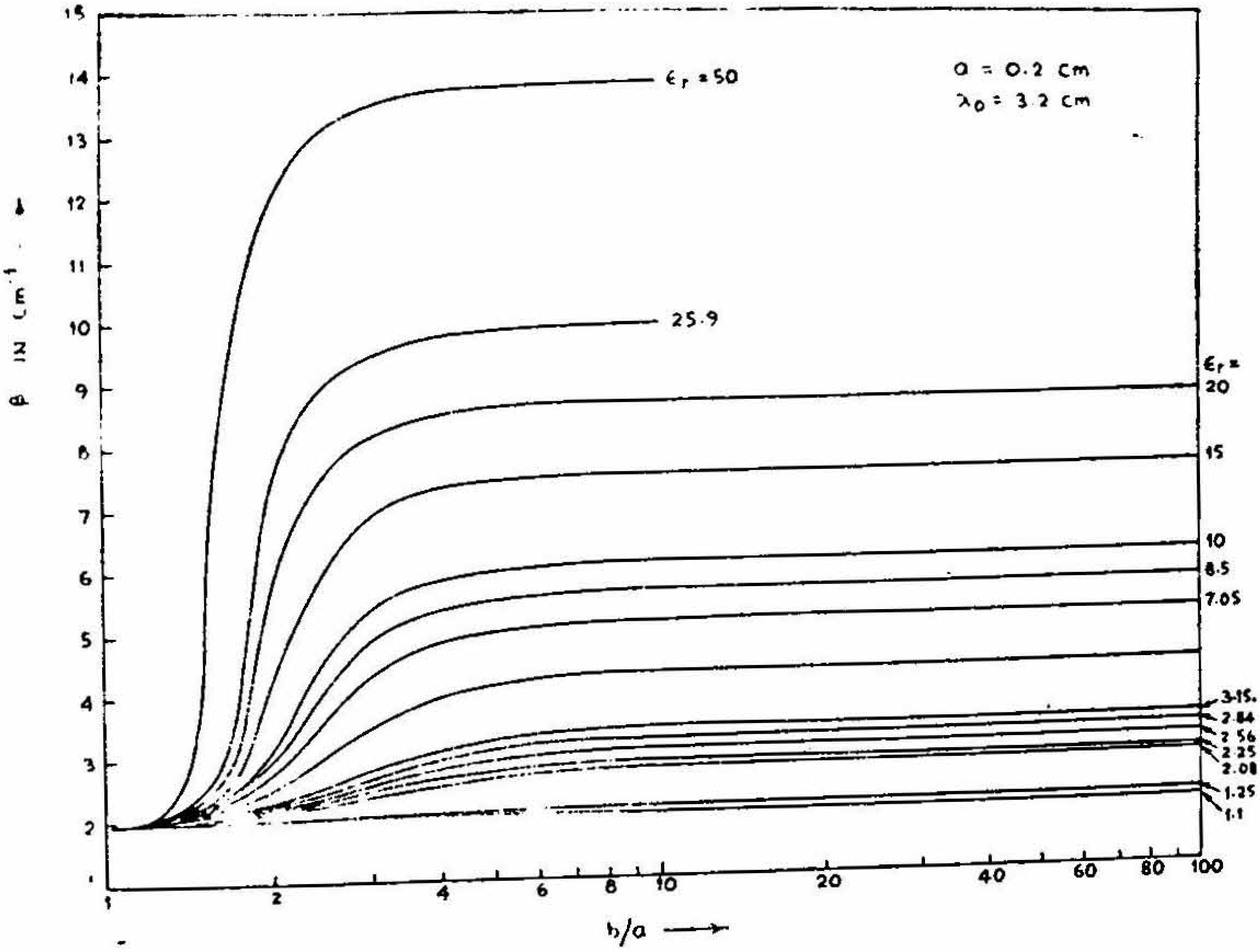

FIG. 8. Variation of the phase constant (β) with b/a ratio.

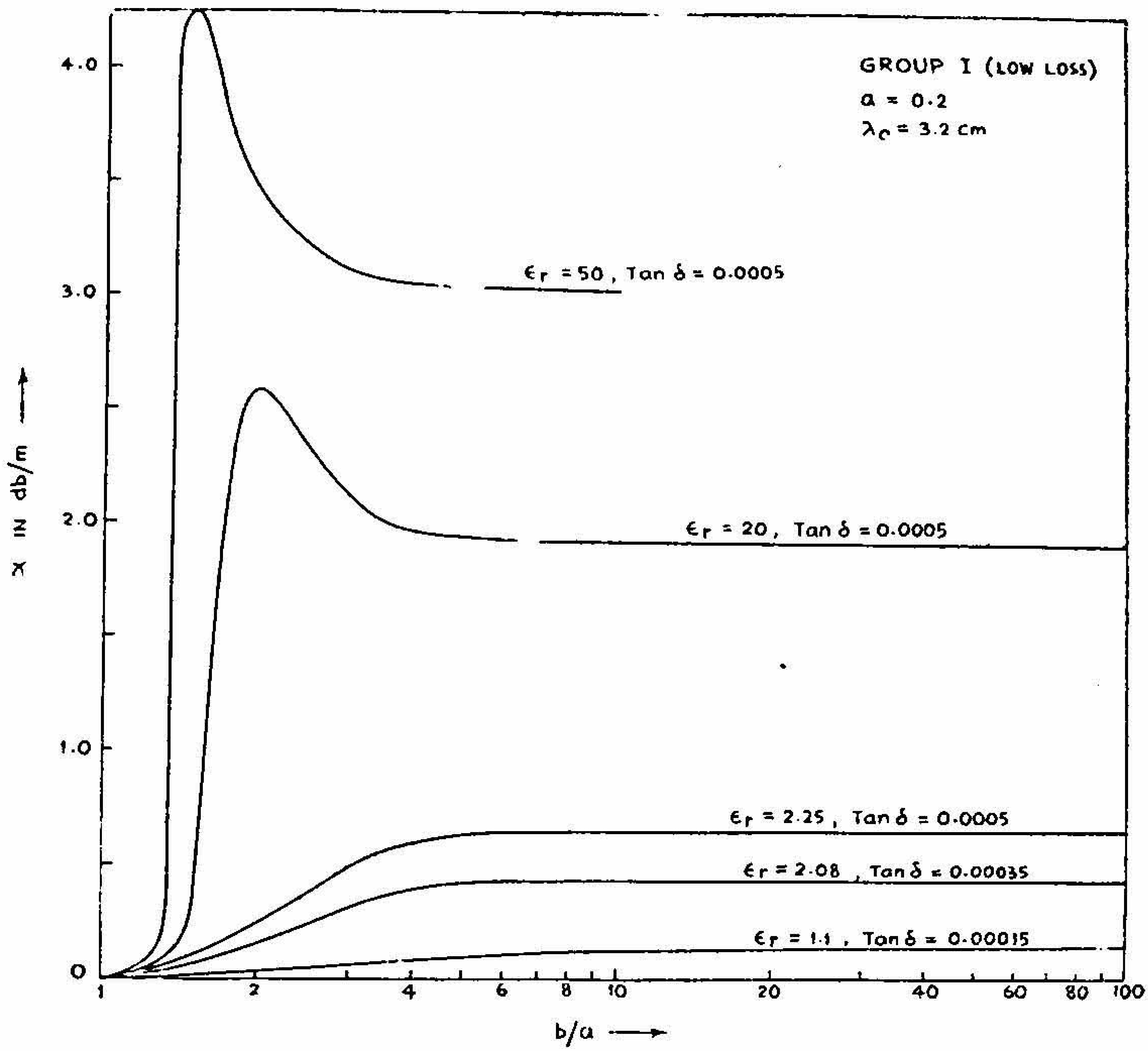

FIG. 9 (*a*). Variation of the attenuation constant (α) with b/a ratio.

The Guide Wavelength

After determining the phase constant β, the guide wavelength is calculated from the relation $\lambda_g = 2\pi/\beta$.

Fig. 11 shows the variation of the guide wavelength ($\lambda g/\lambda_0$) and the phase velocity (v_p/c) with b/a ratio.

7. THE PHASE VELOCITY

The phase velocity 'v' is given by $v = \omega/\beta$. Normalizing v with respect to 'c', the velocity of light

$$\frac{v}{c} = \frac{\omega}{\beta c} = \frac{k_0}{\beta} = \sqrt{\frac{k_0^2}{\beta^2}}$$

$$= \sqrt{\frac{h_1^2 + g_1^2 - g_2^2}{b^2(\epsilon_r - 1)\left[k_0^2 + \frac{g_1^2 - g_2^2}{b^2}\right]}}$$

$$\cdot \left[\frac{h_1^2 + g_1^2 - g_2^2}{h_1^2 + \epsilon_r (g_1^2 - g_2^2)}\right]^{\frac{1}{2}}. \tag{7.1}$$

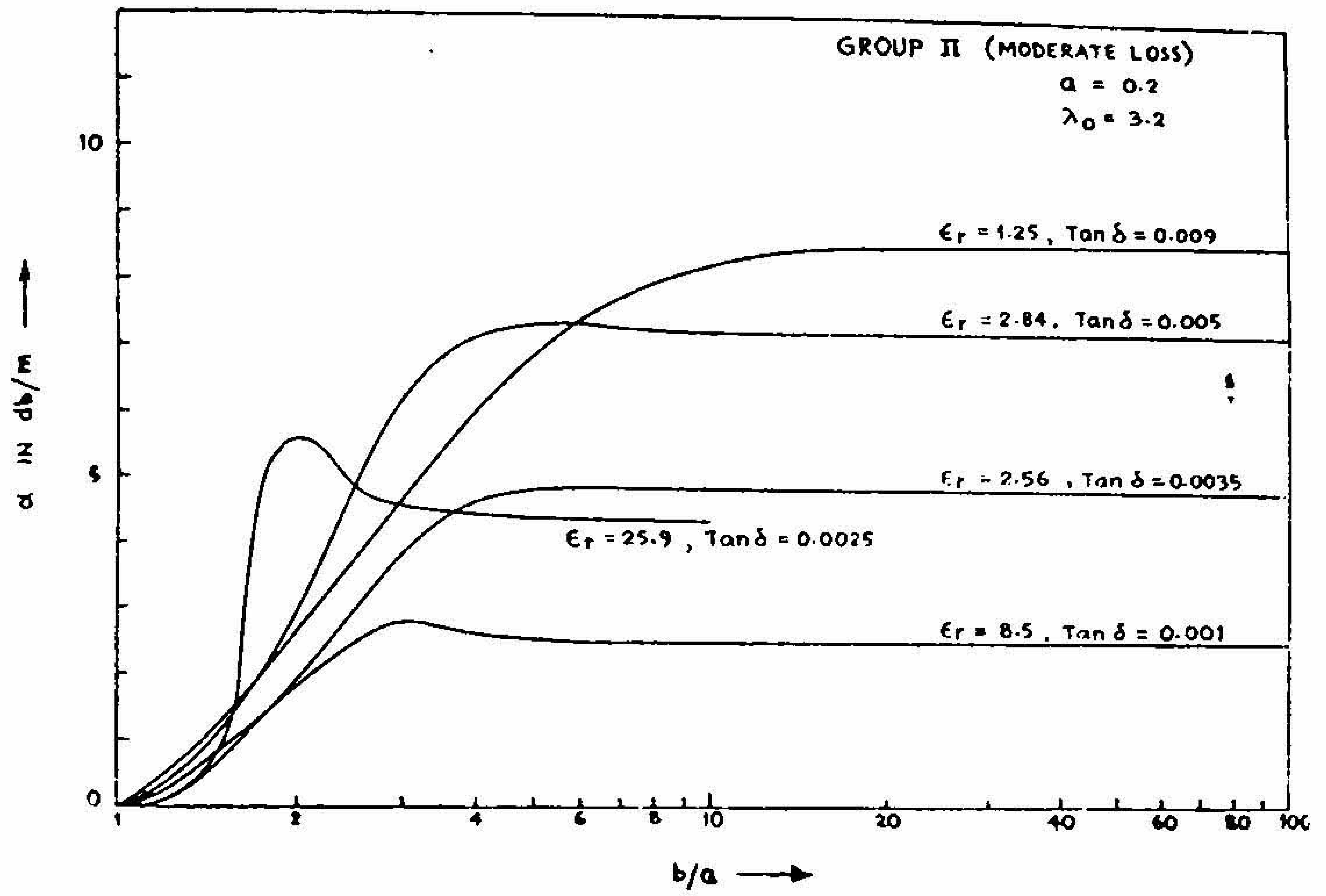

FIG. 9 (*b*). Variation of the attenuation constant (α) with b/a ratio.

8. Power Flow

The power launched in the dielectric-coated metal rod will be transmitted entirely in the longitudinal direction Z, when there is no radiation and the dielectric-coated metal rod acts entirely as a surface waveguide. But if some power is lost by radiation, the power flow will take place not only in the Z-direction but also in the radial (ρ) and azimuthal directions. In the most general case where all the six field components are existing, the power flow in the ρ, ϕ' and z directions is given by

$$\left.\begin{aligned} P_\rho &= \tfrac{1}{2} \, Re \int \int_S [E_{\phi}' \, H_z^* - E_z H_{\phi'}^*] \, \rho d\phi' \, dz \\ P_\phi &= \tfrac{1}{2} \, Re \int \int_S [E_z H_\rho^* - E_\rho H_z^*] \, d\rho dz \\ \text{and} \\ P_z &= \tfrac{1}{2} \, Re \int \int_S [E_\rho H_{\phi'}^* - E_\phi' \, H_\rho^*] \, \rho d\rho dz \end{aligned}\right\} \tag{8.1}$$

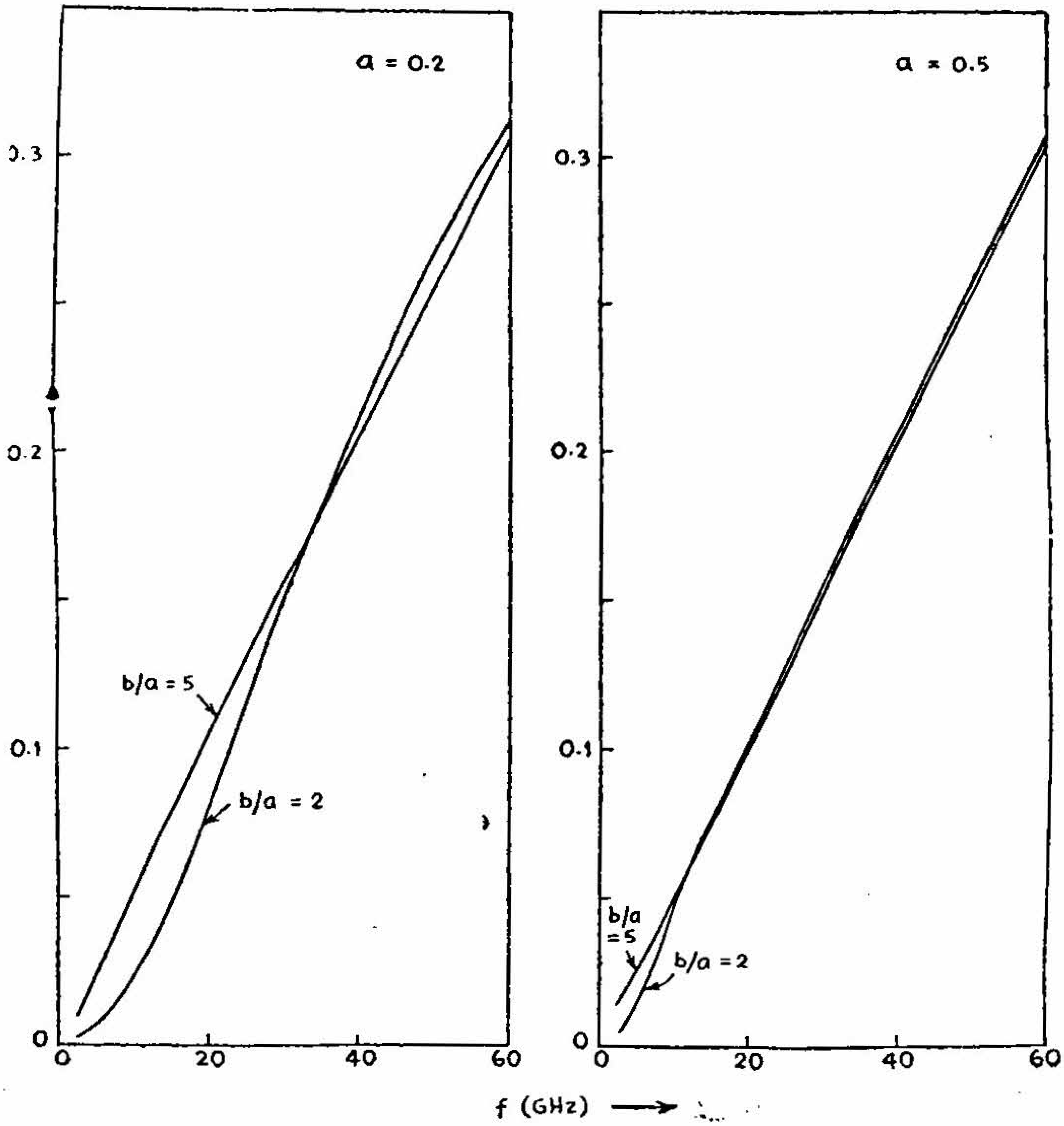

FIG. 10. Variation of the attenuation constant (α) with frequency. $\epsilon_r = 2 \cdot 56$.

where S represents the surface normal to the direction of propagation. But in the present case

$$P_{\phi'} = 0 \text{ since } H_\rho,\ H_z \text{ are non-existing.}$$

It so happens that, P_ρ turns out to be purely reactive. P_z simplifies to

$$P_z = \tfrac{1}{2} \int \int_S E_\rho H_{\phi'}^* \ \rho d\rho dz.$$

This expression is obtained by directly integrating the Poynting Vector over the cross-section.

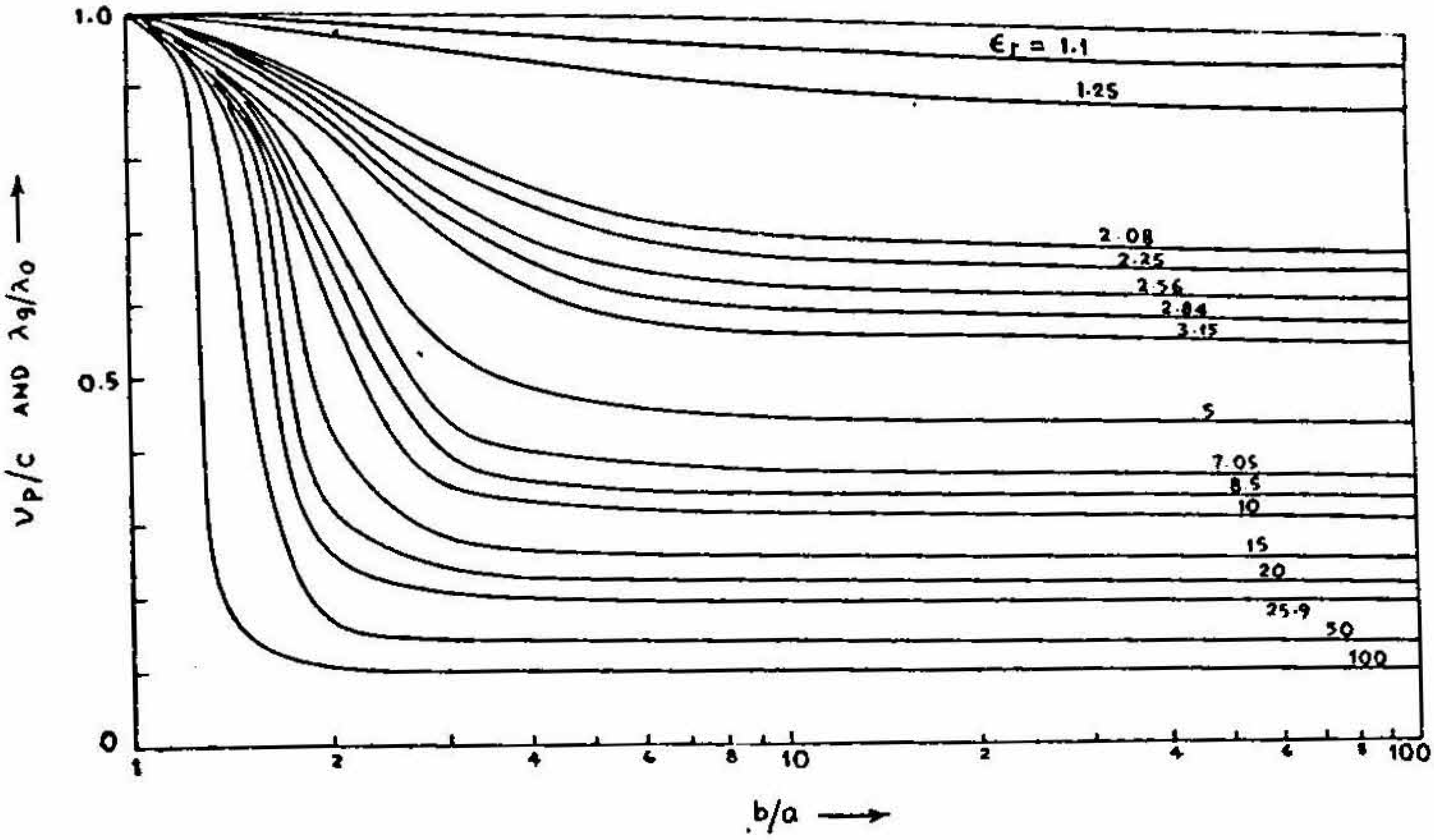

FIG. 11. Variation of the guide wavelength (λ_g/λ_0) and the phase velocity (v_p/c) with b/a ratio. $a = 0{\cdot}2$ cm.

While calculating the power flow we make the following assumptions: (a) the distortion of the field in the dielectric layer due to the finite conductivity of the conductor is neglected, *i.e.*, $G = 0$ in equations (4.1) and (4.2). It may be mentioned here that this assumption is also usually made in calculating the power in hollow waveguides, (b) the field strengths are assumed to be given by their effective values.

The Field Components in the region ($a \leqslant \rho \leqslant b$) are

$$\left.\begin{aligned} E_z &= A\left[J_0(\xi) - \frac{J_0(u)}{Y_0(u)}\, Y_0(\xi)\right] \exp(-\gamma z) \\ &= A\left[P(\xi)/Y_0(u)\right] \exp(-\gamma z) \\ H_{\phi'} &= \frac{-j\omega\epsilon_2 b}{h}\, A\, \frac{P'(\xi)}{Y_0(u)} \exp(-\gamma z) \end{aligned}\right\} \tag{8.2}$$

and

$$E_\rho = \frac{-\rho}{\omega\epsilon_2} H_{\phi'}$$

where

$$\xi = \frac{h\rho}{b}, \quad u = h/\sigma.$$

Outside the dielectric layer $(\rho > b)$

$$\left.\begin{aligned} E_z &= CK_0(\psi)\exp(-\gamma_z) \\ H_{\phi'} &= \frac{j\omega\epsilon_0}{g} bCK_0'(\psi)\exp(-\gamma_z) \\ E_\rho &= p/\omega\epsilon_0 H_{\phi'} \end{aligned}\right\} \qquad (8.3)$$

where

$$\psi = g\rho/b.$$

The mean power which is propagated in the z-direction in the dielectric layer is

$$P_2 = P_{2z} = \int_{\phi'=0}^{2\pi} \int_{\rho=a}^{b} E_\rho \times H_\phi{}^* \rho d\rho d\phi'$$

$$= 2\pi \int_{\rho=a}^{b} \frac{-p}{\omega\epsilon_2} \mid H_\phi \mid^2 \rho d\rho$$

$$= -2\pi p \int_{\rho=a}^{b} -(\omega\epsilon_2)\frac{b^2}{h^2} A^2 \frac{P'^2(\xi)}{Y_0{}^2(u)} \rho d\rho d\phi'. \qquad (8.4)$$

Let

$$E_0 = \frac{AP(h)}{Y_0(u)} = CK_0(g)$$

be the effective value of the longitudinal electric field component at $\rho = b$.

Also

$$\xi = \frac{h\rho}{b}$$

at

$$\rho = b, \quad \xi = h$$

at

$$\rho = a, \quad \xi = \frac{ha}{b} = h/\sigma = u$$

$$\xi = h\rho/b, \quad d\xi = \frac{hd\rho}{b}$$

$$\rho d\rho = \frac{b^2}{h^2}\xi d\xi.$$

Hence

$$P_2 = P_{2z} = 2\pi \int_u^h p\omega\epsilon_2 \frac{b^2}{h^2} A^2 \frac{P'^2(\xi)}{Y_0^2(u)} \frac{b^2}{h^2} \xi d\xi$$

$$= 2\pi \frac{b^4}{h^4} p\omega\epsilon_2 \frac{E_0^2}{p^2(h)} \int_u^h p'^2(\xi) \xi d\xi$$

$$= 2\epsilon \left\{\frac{\pi b^4 pk_0}{\eta_0} E_0^2\right\} \frac{1}{h^4 P^2(h)} \int_u^h P'^2(\xi) \xi d\xi. \tag{8.5}$$

The indefinite integral

$$\int \xi P'^2(\xi) d\xi$$

$$= \frac{1}{2} \xi^2 \left[P^2(\xi) + \frac{2}{\xi} P(\xi) P'(\xi) + P'^2(\xi)\right].$$

Hence

$$\int_u^h \xi P'^2(\xi) d\xi = \tfrac{1}{2} h^4 P^2(h) N(h)$$

where

$$N(h) = f^2(h)[1 - R(h)] + [2f(h) + 1] \frac{1}{h^2}. \tag{8.6}$$

The power carried by the dielectric layer will hence simplify to

$$P_2 = P_2(z) = 2\epsilon_r P_0 \frac{1}{h^4 P^2(h)} \frac{1}{2} h^4 P^2(h) N(h) \tag{8.7}$$

$$P_2 = P_{2z} = \epsilon_r N(h) P_0 \tag{8.8}$$

where

$P_0 = \dfrac{\pi b^4 pk_0 E_0^2}{\eta_0}$ is the unit power.

In the region outside the dielectric ($\rho > b$), we calculate the power transmitted outside a cylinder (coaxial with the surface waveline) of radius

$\rho = qb \; (q \geqslant 1)$

$$P_3 = P_{3z} = \int_\rho^\infty \int_{\phi'=0}^{2\pi} E_\rho H_{\phi'}^* \, \rho d\rho d\phi' \tag{8.9}$$

$$= 2\pi \int_\rho^\infty \frac{p}{\rho\omega\epsilon_0} (\omega\epsilon_0)^2 \frac{b^2}{g^2} C^2 K_0'^2(\psi) \rho d\rho$$

$$\psi = g\rho/b, \quad d\psi = \frac{g}{b} d\rho$$

$$\rho d\rho = \frac{b^2}{g^2} \psi d\psi.$$

As

$$\rho \to \infty, \quad \psi \to \infty.$$

At

$$\rho = qb, \quad \psi = qg.$$

Hence

$$P_3 = P_{3z} = 2\pi p \omega \epsilon_0 \frac{b^2}{g^2} C^2 \int_{qg}^{\infty} K_0'^2 (\psi) \psi d\psi. \tag{8.10}$$

So

$$P_3 = P_{3z} = \frac{2\pi p \omega \epsilon_0 b^4}{g^4} \frac{E_0^2}{K_0^2 (g)} \int_{qg}^{\infty} K_0'^2 (\psi) \psi d\psi$$

$$= 2\left[\frac{\pi b^4 pk}{\eta} E_0^2\right] \frac{1}{g^4 K_0^2 (g)} \int_{qg}^{\infty} K_1^2 (\psi) \psi d\psi. \tag{8.11}$$

The indefinite integral

$$\int K_1^2 (\psi) \psi d\psi = \tfrac{1}{2} K_1^2 (\psi) \psi^2 - \psi K_1 (\psi) K_0 (\psi) - \tfrac{1}{2}\psi^2 K_0^2 (\psi) \tag{8.12}$$

After some simplification, this reduces to

$$\int K_1^2 (\psi) \psi d\psi = \frac{-1}{2} \psi^4 K_0^2 (\psi) L (\psi)$$

where

$$L (g) = - \phi^2 (g) + [2\phi (g) + 1] \frac{1}{g^2}$$

and

$$\phi (g) = \frac{1}{g} \frac{K_1 (g)}{K_0 (g)}$$

$$\int_{qg}^{\infty} K_1^2 (\psi) \psi d\psi = \left[\frac{-\psi^4}{2} K_0^2 (\psi) L (\psi)\right]_{qg}^{\infty}. \tag{8.13}$$

As $\psi \rightarrow \infty$, the above integral varies as and hence tends to zero.

$$P_3 = P_{3z} = 2P_0 \frac{1}{g^4 K_0^2(g)} \frac{(qg)^4}{2} K_0^2(qg)\, L(qg). \tag{8.14}$$

In the particular case where we are interested in the power transmitted outside the dielectric-coating (Medium III) $\rho = b,\ q = 1$.

Hence

$$P_3 = P_3(z) = P_0 L(g).$$

The total power carried by the wave is

$$P = P_{2z} + P_{3z} = P_2 + P_3 = P_0\,[\epsilon_r N(h) + L(g)]. \tag{8·15}$$

Fig. 12 shows the variation of the power carried by the dielectric layer with $b|a$ ratio.

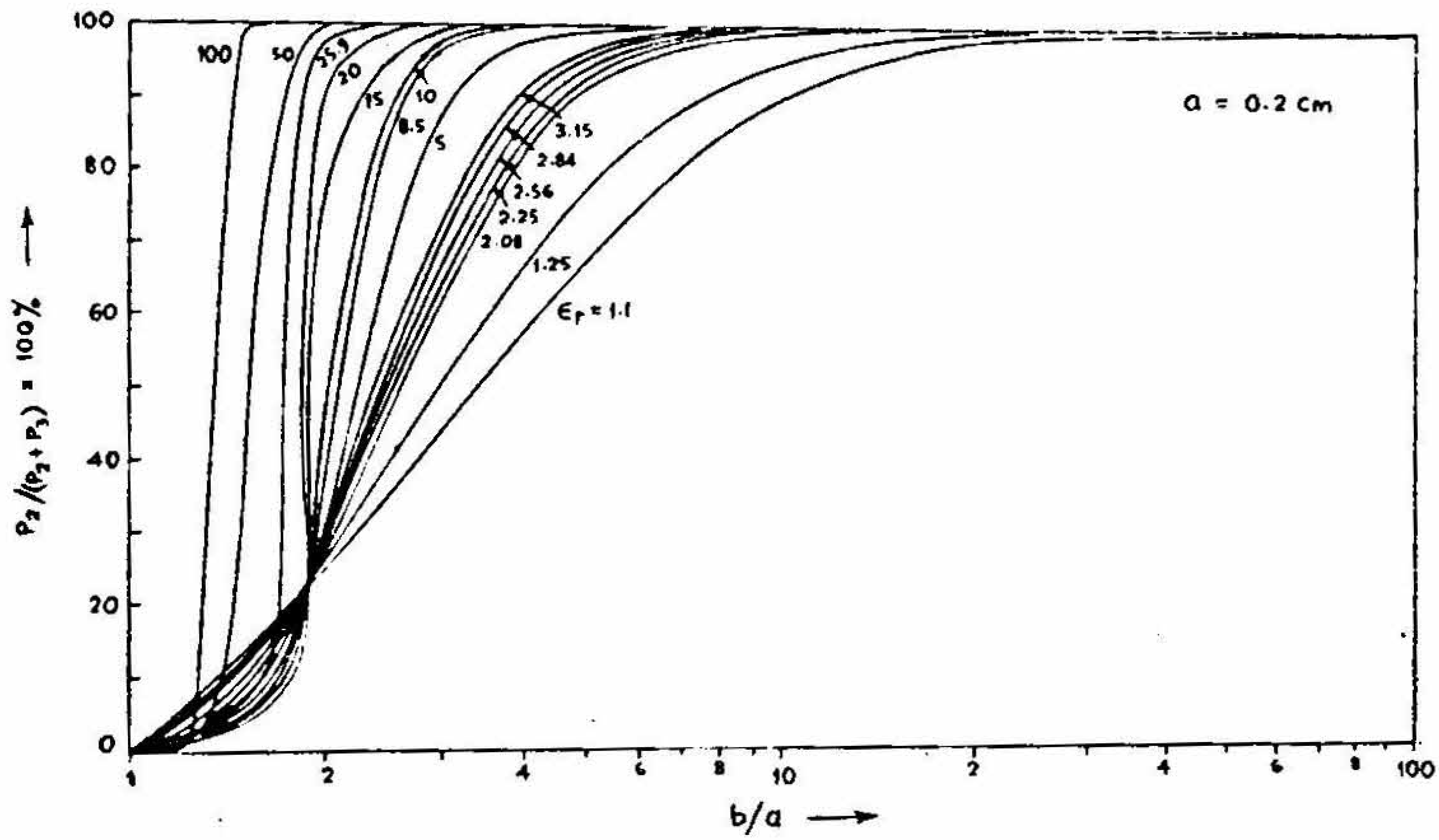

FIG. 12. Variation of the power carried by the dielectric layer with b/a ratio.

Fig. 13 shows the variation of the power travelling outside dielectric layer with b/a ratio.

Fig. 14 shows the variation of the relative power distribution (power propagating inside and power propagating outside) with frequency.

Fig. 15 shows the constant percentage power contours.

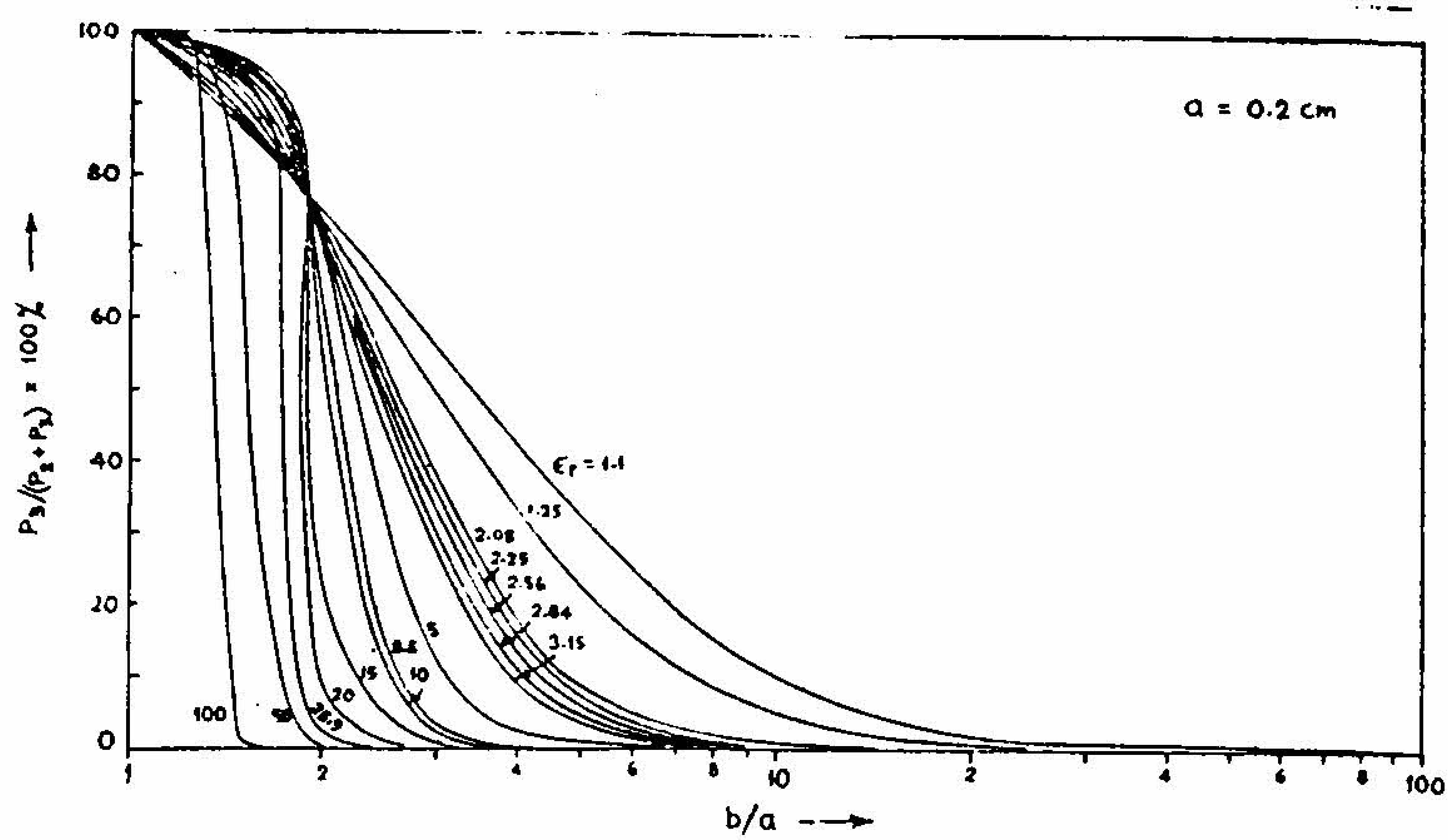

FIG. 13. Variation of the power travelling outside the dielectric layer with b/a ratio.

9. MAXIMUM POWER HANDLING CAPACITY

When transmitting pulse signals of large duty ratic, the maximum power is determined by the electrical breakdown in the region of maximum field intensity. Since air breaks down earlier than solid dielectrics, if the surrounding medium is ai., the maximum permissible field strength in medium 3 is $\hat{E}$, the breakdown field strength for air.

The electrical field strength is a maximum at the surface of the dielectric ($\rho = b$) where the two field components E_ρ and E_z are in phase quadrature. The ratio of their absolute values is

$$\frac{|E_\rho|}{|E_z|} = \frac{bp}{g}\frac{K_1(g)}{K_0(g)} = bp\phi(g). \tag{9.1}$$

This ratio is larger than unity for all values of the surface wave line parameters and we must take $E_{\rho\max} = E_{\max}$. The maximum value of the conventional unit power P_0 using (9.1) is

$$P_{0\max} = \frac{\pi b^2 k_0}{2p\eta_0\phi^2(g)} E_\rho{}^2{}_{\max}. \tag{9.2}$$

By substituting this value of P_0 in equation (8.15), we obtain the total breakdown power.

$$P_{\max} = \frac{\pi b^2}{2\eta_0}\frac{k_0}{\rho}\frac{\{\epsilon_r N(h) + L(g)\}}{\phi^2(g)} E^2_{\rho\max}. \tag{9.3}$$

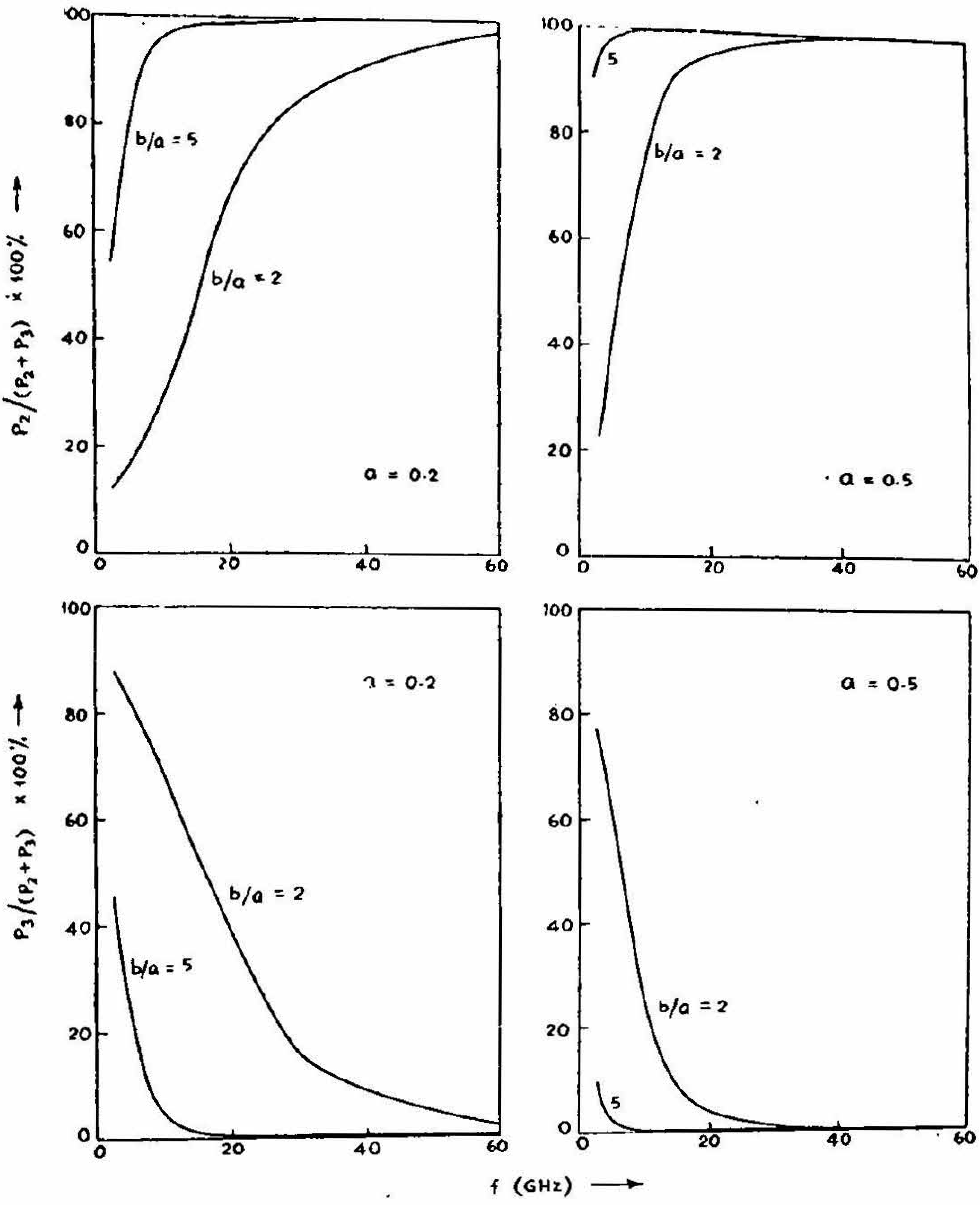

FIG. 14. Variation of the relative power distribution (power propagating inside and power propagating outside) with frequency. $\epsilon_r = 2 \cdot 56$.

Fig. 16 shows the variation of the power handling capacity (P_{max}) with b/λ_0.

Fig. 17 shows the variation of the power handling capacity (P_{max}) with frequency.

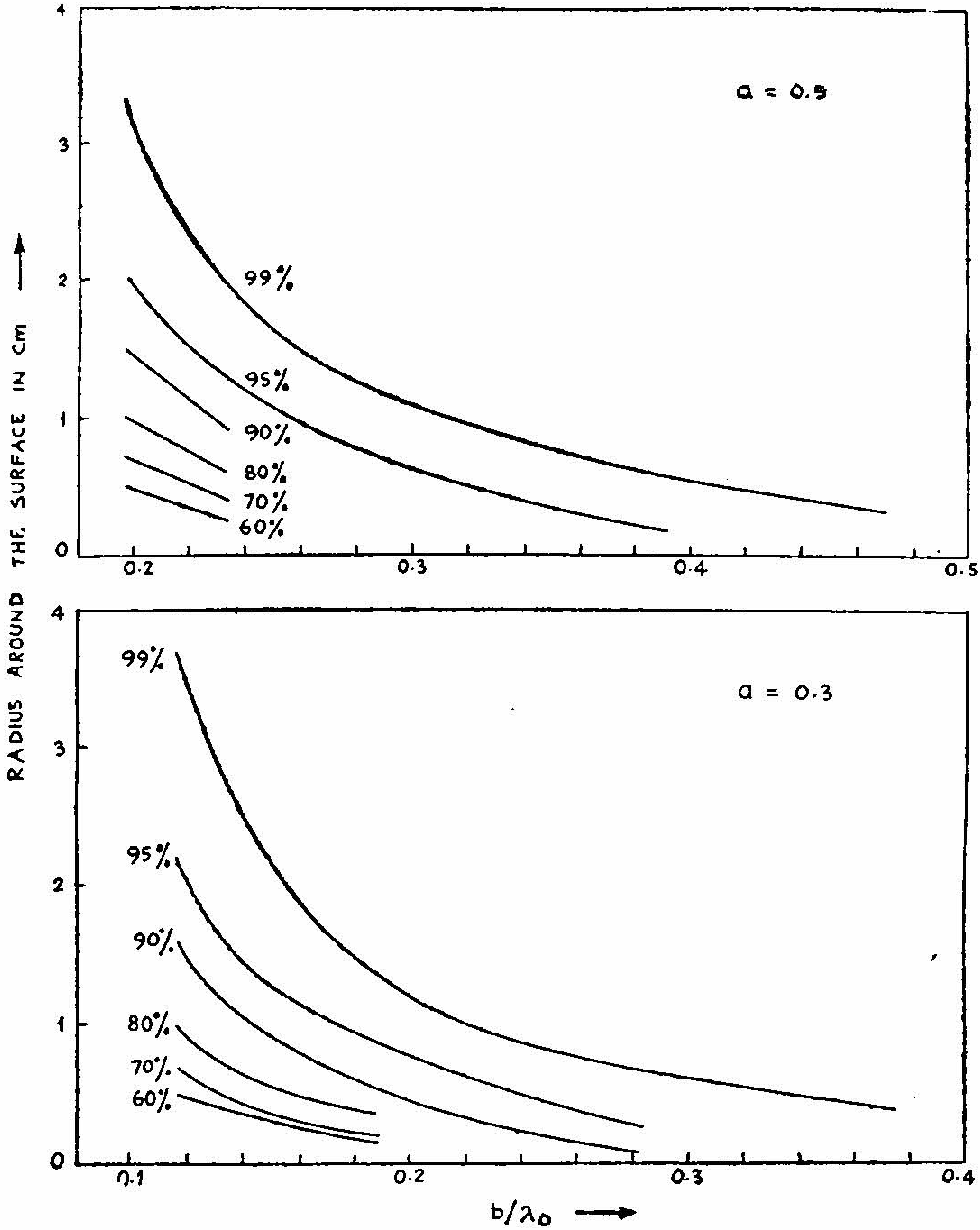

FIG. 15

10. CHARACTERISTIC IMPEDANCE AND SURFACE IMPEDANCE

The characteristic impedance of a surface wave line is usually defined as the ratio of the total transmitted power to the square of the current I_a flowing in the inner conductor

$$P = I_a{}^2 Z_a = [2\pi_a H_\phi{}' (a)]^2 Z_a. \tag{10.1}$$

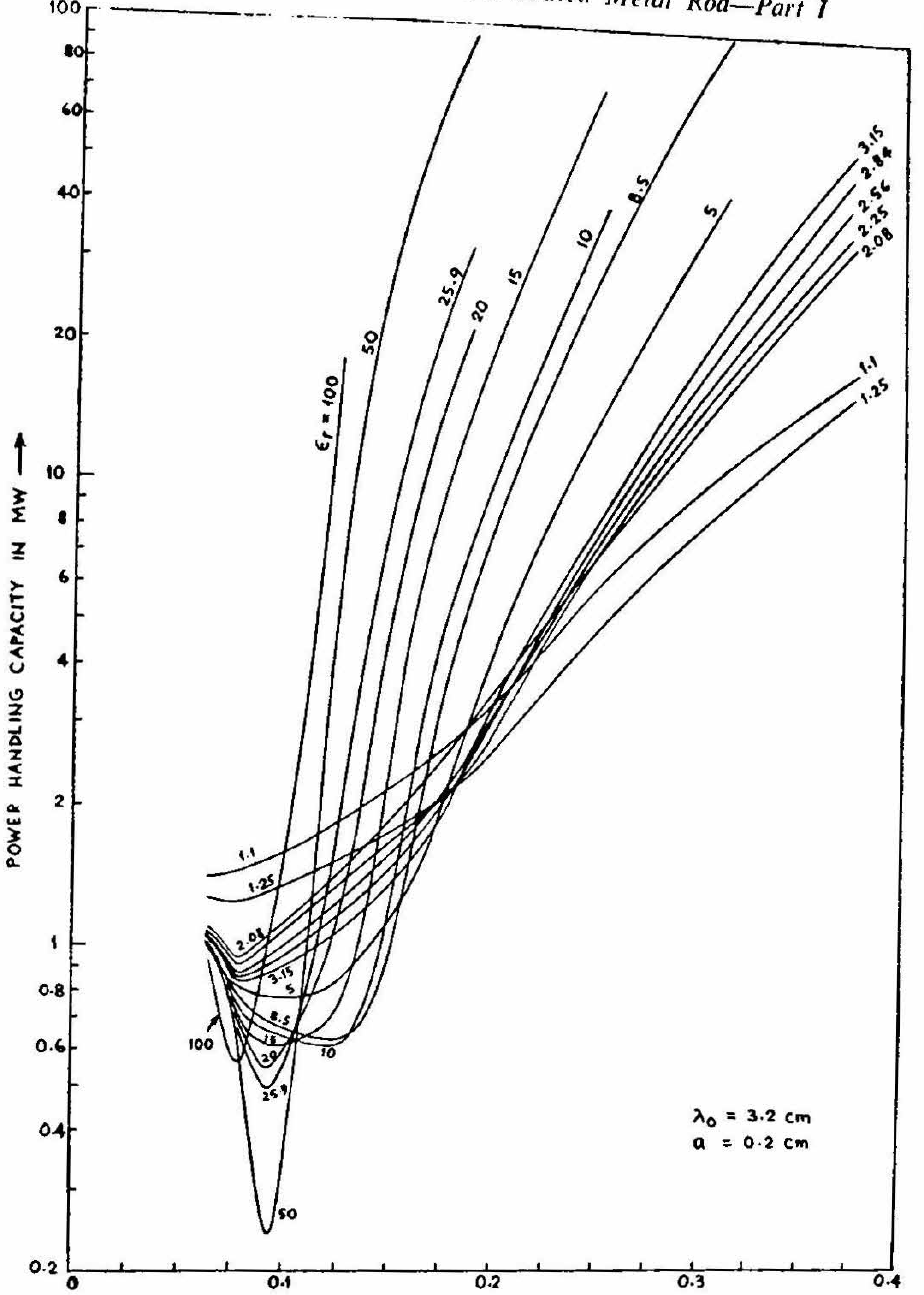

FIG. 16. Variation of the power handling capacity (P_{max}) with b/λ_0.

We can also have another definition based on the equivalent current I_b in the external surface of the dielectric.

$$P_b = I_b^2 Z_b = [2\pi b H_{\phi'}(b)] Z_b. \tag{10.2}$$

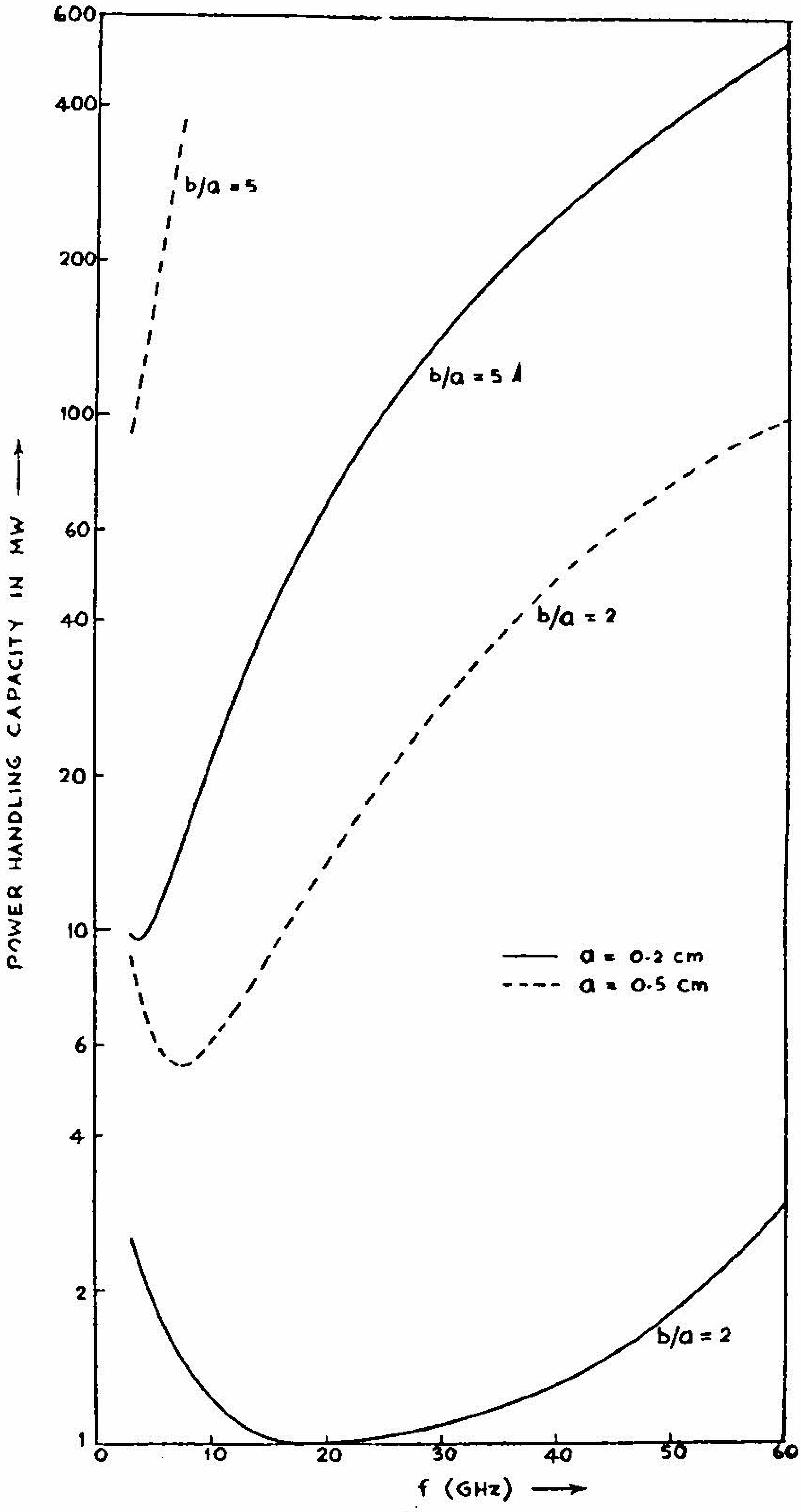

FIG. 17. Variation of the power handling capacity (P_{max}) with frequency. $\epsilon_r = 2 \cdot 56$.

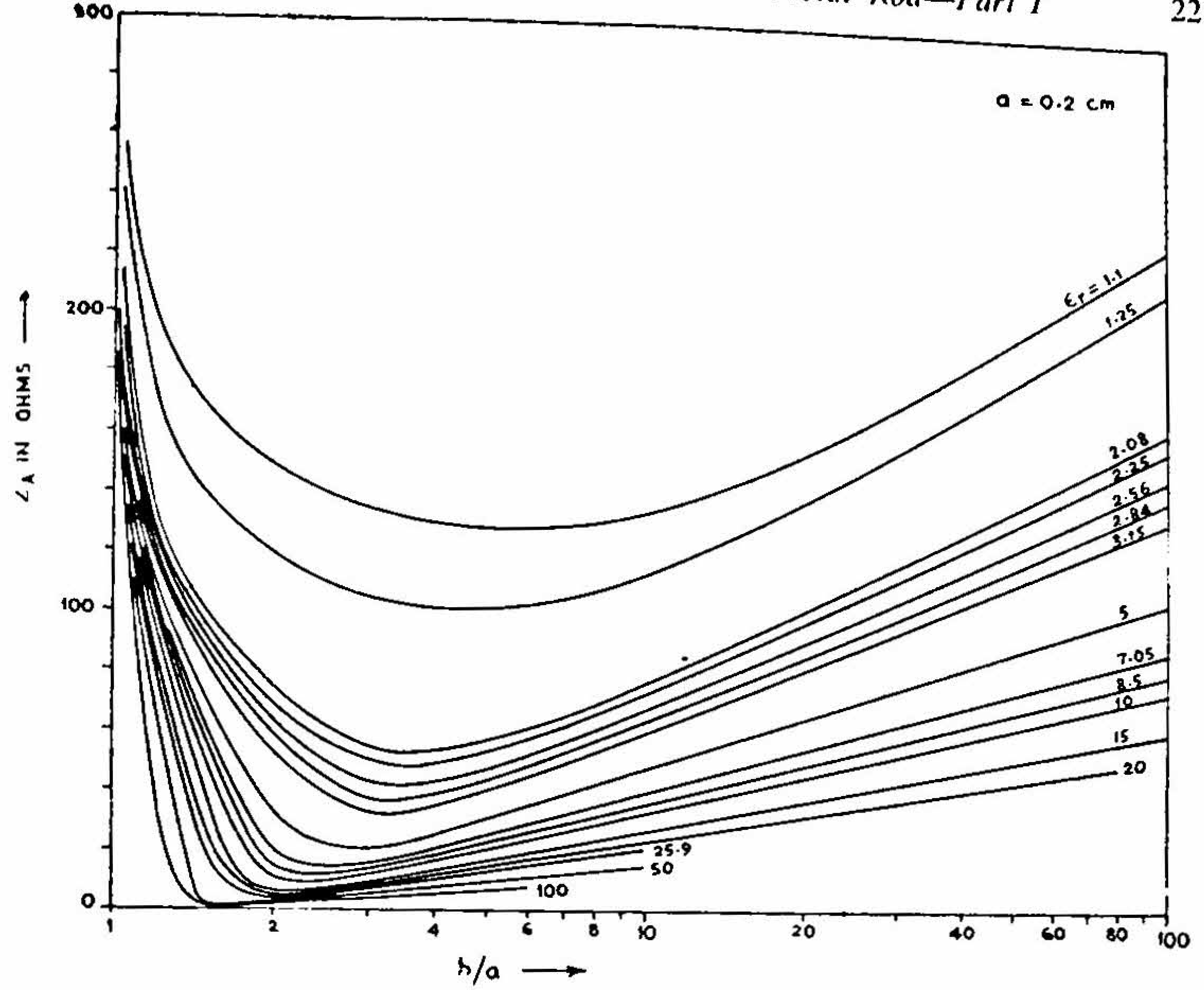

FIG. 18. Variation of the characteristic impedance (Z_A) with b/a ratio.

The difference between these two definitions becomes appreciable as the dielectric coating thickness increases. Substituting (10.1) and (10.2) in equation (8.15), we obtain

$$Z_a = \frac{\pi b}{16 \epsilon_r^2} \frac{p}{k} [h^2 P(h)]^2 [\epsilon_r N(h) + L(g)] \tag{10.3}$$

$$Z_b = \frac{\eta}{4\pi} \frac{p}{k} \frac{[\epsilon_r N(h) + L(g)]}{\epsilon_r^2 f^2(h)} \simeq \frac{\eta}{4\pi} \frac{p}{k} \frac{[\epsilon_r N(h) + L(g)]}{\phi^2(g)} . \tag{10.4}$$

The surface impedance Z_s is defined as the ratio of the tangential components of the electric and magnetic fields on the outer boundary of the dielectric. From equation (3.3).

$$Z_s = \frac{E_z}{H_{\phi'}} = \frac{j\eta}{\epsilon_r b k f(h)} . \tag{10.5}$$

Figs. 18 and 19 show the variation of the characteristic impedance Z_A with b/a ratio and a/λ_0 respectively.

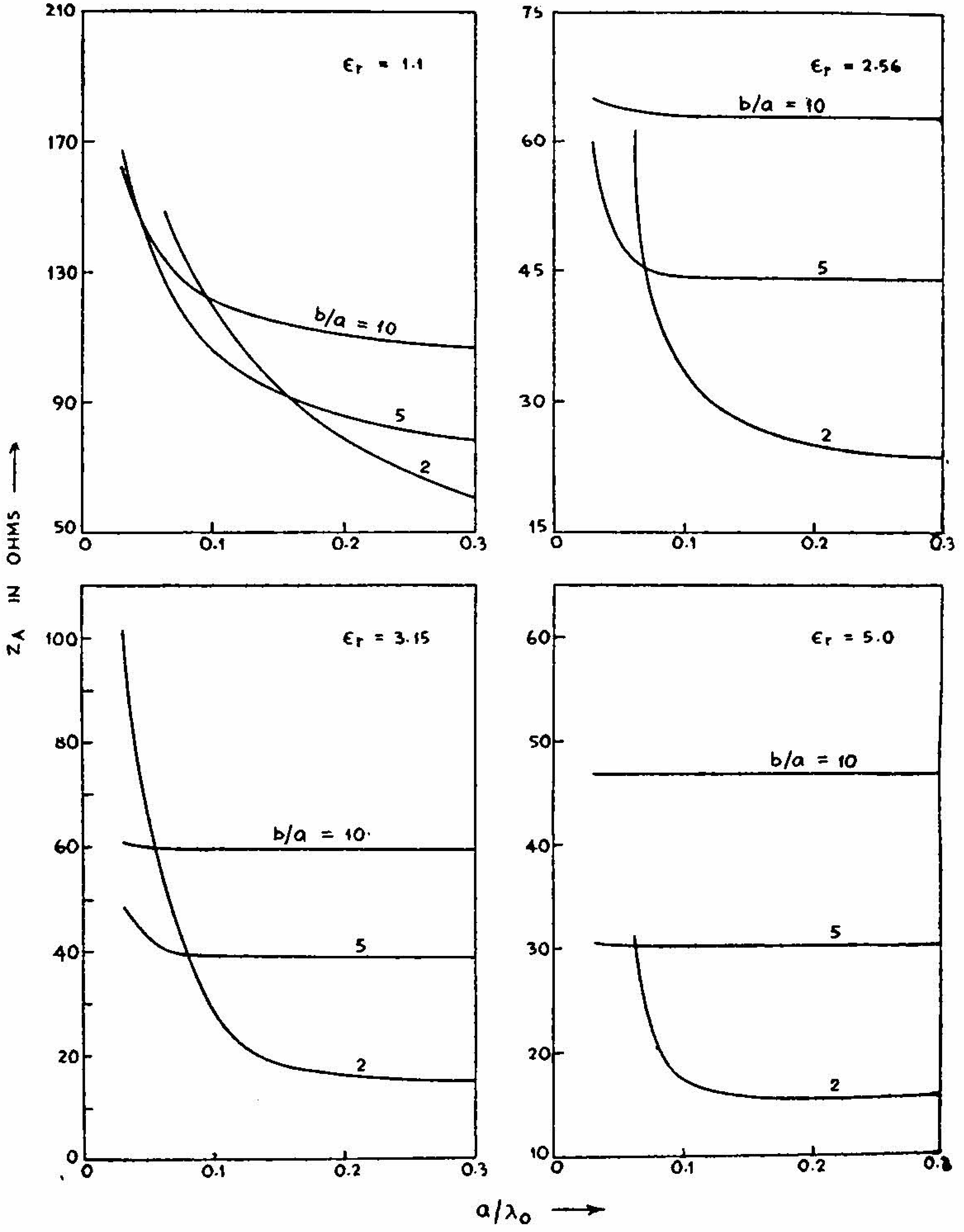

FIG. 19. Variation of the characteristic impedance (Z_A) with a/λ_0. $\lambda_0 = 3 \cdot 2$ cm.

Figs. 20 and 21 show the variation of the surface resistance R_s with b/a ratio and frequency respectively.

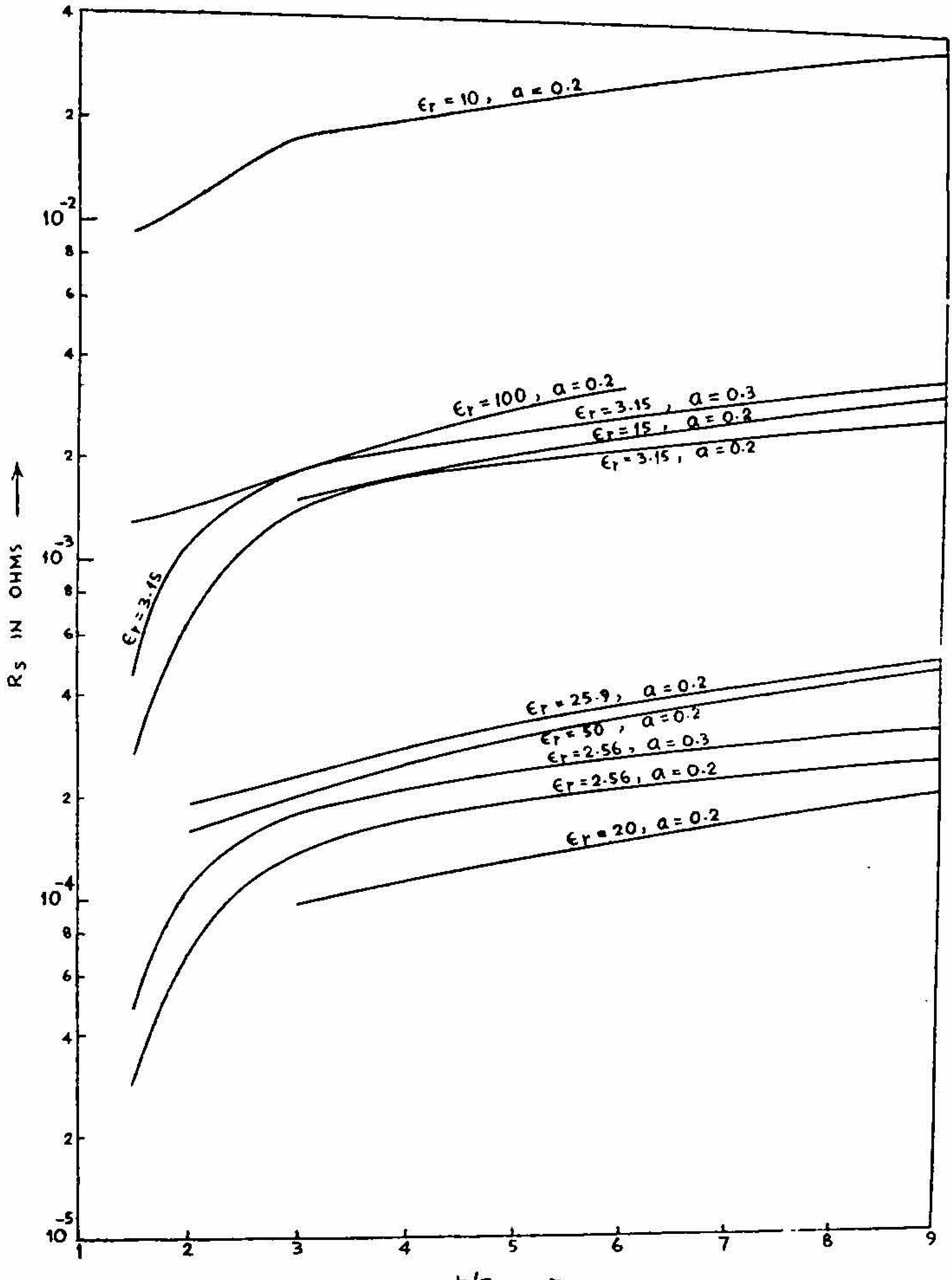

FIG. 20. Variation of the surface resistance (Rs) with b/a ratio.

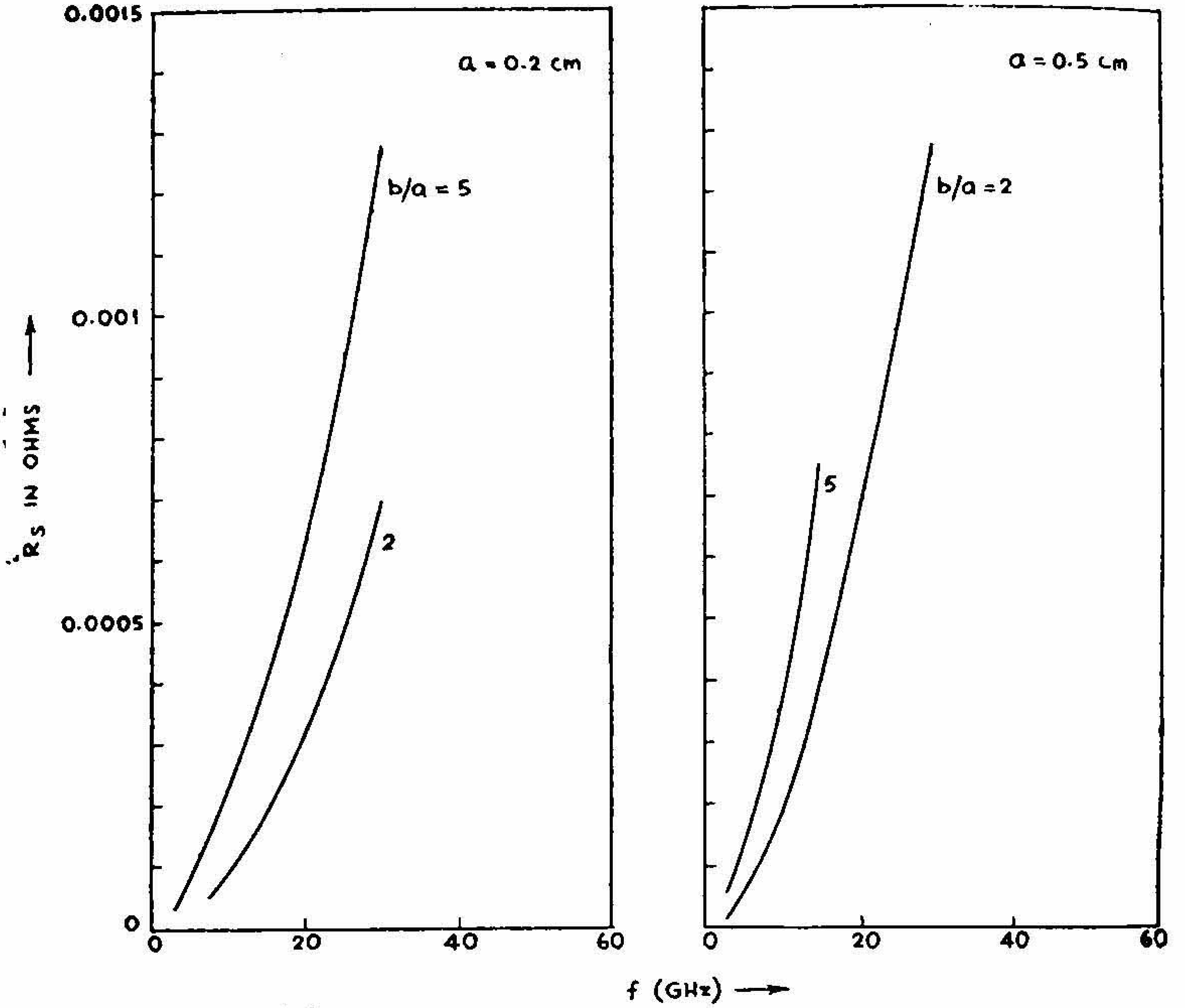

FIG. 21. Variation of the surface resistance (Rs) with frequency. $\epsilon_r = 2 \cdot 56$.

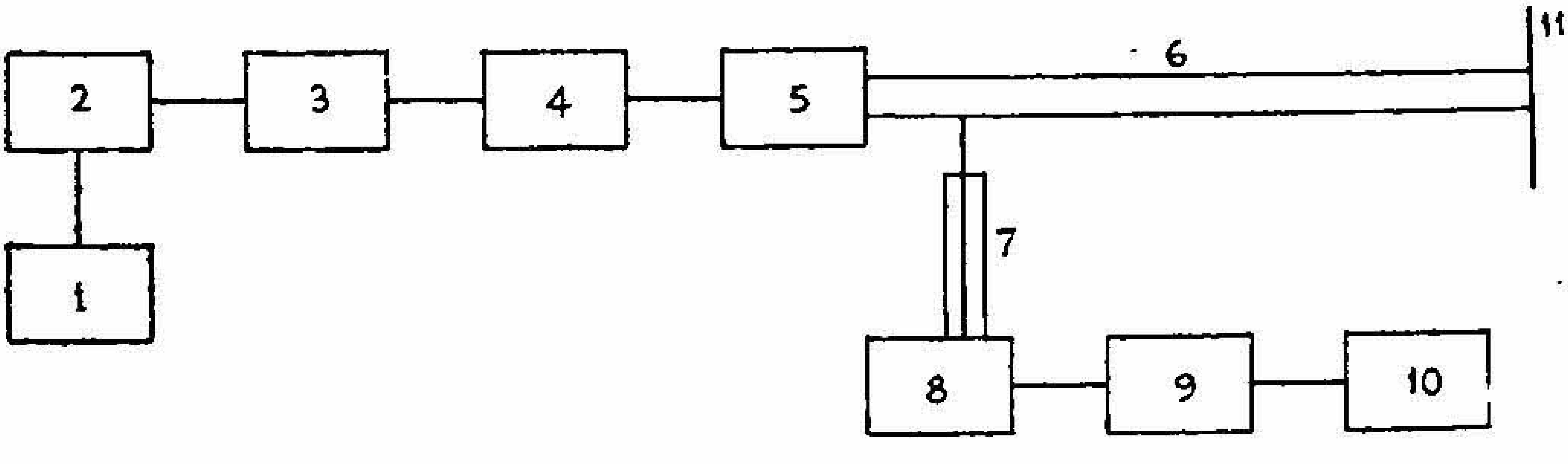

1. REGULATED POWER SUPPLY WITH SQUARE WAVE MODULATOR.
2. 723 A/B KLYSTRON.
3. FLAP ATTENUATOR.
4. FREQUENCY METER.
5. MODE TRANSDUCER.
6. DIELECTRIC-COATED METAL ROD.
7. PROBE.
8. COAXIAL TO RECTANGULAR ADOPTER
9. CRYSTAL MOUNT.
10. DETECTOR AMPLIFIER.
11. SHORTING METALLIC PLATE

FIG. 22.

11. Experimental Set Up for the Measurement of Electric Field Components

The general experimental set up for the measurement of electric field components is shown in Fig. 22.

1. *Feed End of the Guide*

A rectangular guide is excitde in its dominant TE_{10} mode by a 723. $A_{/}B$ Klystron. Using a mode transducer this is converted to the TM_{01} mode on the surface wave line. The mode transducer (Fig. 23) consists of a coaxial adapter and a launching cone. The metallic portion of the surface wave

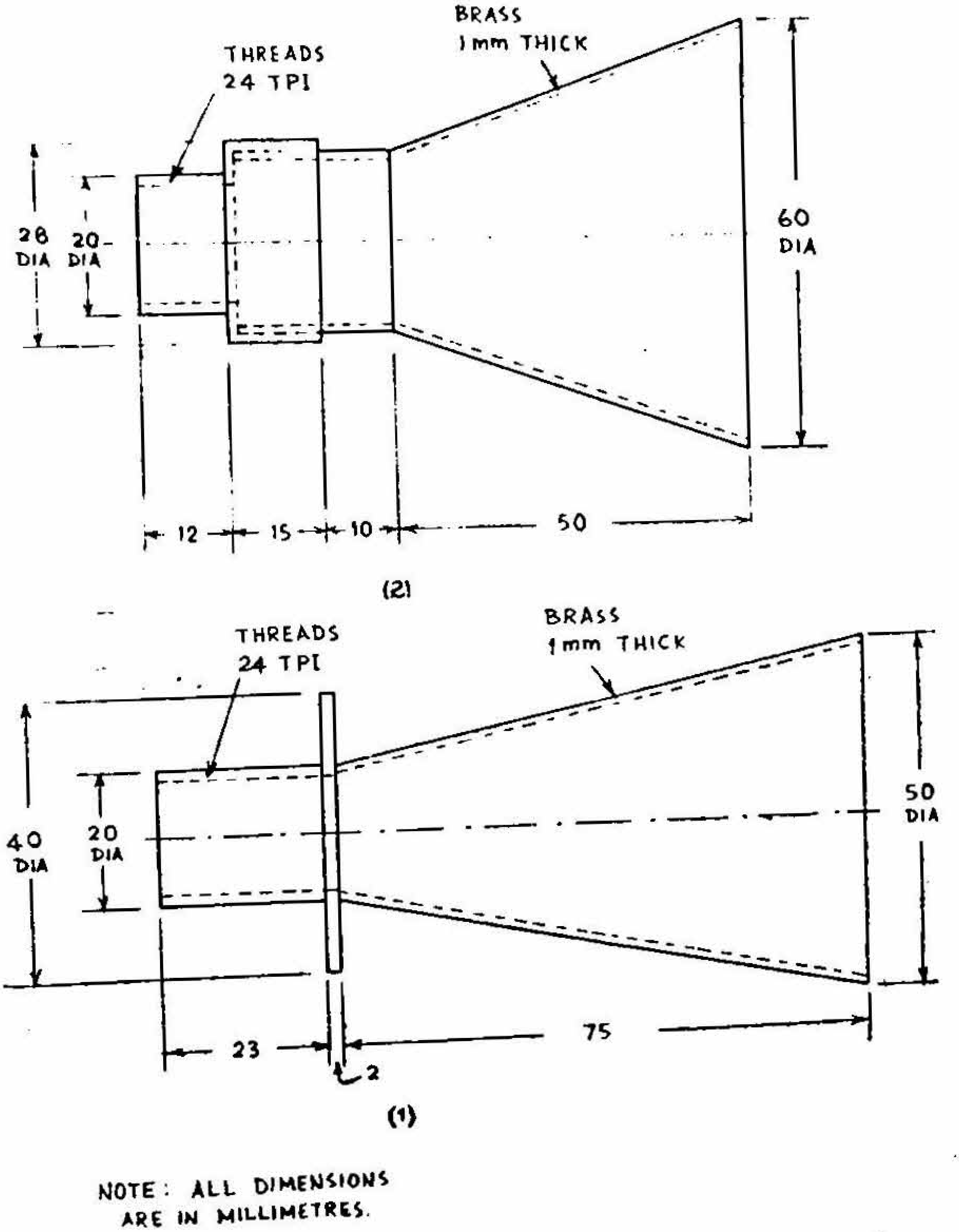

Fig. 23. Constructional details of the cones used with the mode transducers for thin dielectric coatings.

line is tapered and the launching cone is screwed to the adapter. The length of the transition is long enough to ensure a gradual variation of impedance. Since the field configuration of the TM_{01} mode on the dielectric coated conducting cylinder is similar to that of the TEM mode in a coaxial line, this method of excitation gives a fairly good lannching efficiency. The generator is isolated from the mode transducer by an attenuator.

Klystron feed.—The Klystron 723 A/B is mounted directly on the broad-side of a rectangular waveguide, so that the output of the probe of the Klystron protrudes through a hole made at the centre of the broad face into the guide. This enables the excitation of the dominant TE_{10} mode in the rectangular guide. One end of the guide is fitted with an adjustable plunger The plunger and the length of the output probe of the Klystron inside the guide are adjusted for maximum power transfer. The required voltages for the Klystron are given by an electronically stabilized power supply. The reflector is modulated by 1,000 Hz square wave.

2. *The Free End of the Guide*

The length of the guide is about 1·20 meters and it is shorted by a metal plate at the far end. The guide is suspended by means of nylon threads.

3. *Detector System*

The detecting system consists of a $\lambda/4$ or $\lambda/2$ probe connected to a coaxial adopter ard detecting section. The probe along with the accessories is mounted on a probe carriage which has three independent mutually perpendicular motions. The detector amplifier is a selective amplifier with a twin-tee network tuned to $1 K Hz$, the frequency of the square-wave with which the reflector voltage of the klystron is modulated.

Measurement of Electric Field Components.—The probe is set paralled to the electric field component that is being measured, close to the surface of the rod, almost touching it. The reflector voltage, the amplitude and the frequency of the square wave are tuned for the maximum detector reading. The position of the probe is noted down on a scale provided for the purpose. The probe is then moved in steps of 1 mm in the z-direction and each time the d.c. μ A reading is noted. As we move the probe in the longitudinal direction parallel to z-axis, we get the standing wave pattern from which the guide wavelength is determined by finding out the distance between two consecutive maxima or minima and multiplying it by 2. A dipole probe is used for measurement of E_z and a $\lambda/4$ probe is used for E_ρ. Next the probe is moved in the radial direction in steps of 1 mm and each time the d.c. microammeter reading is noted down which gives the radial decay of the field component.

Figs. 24 and 25 show the calculated and measured β and λ_g/λ_0 *vs.* b/a.

Fig. 26 shows the radial field decay (both calculated and measured).

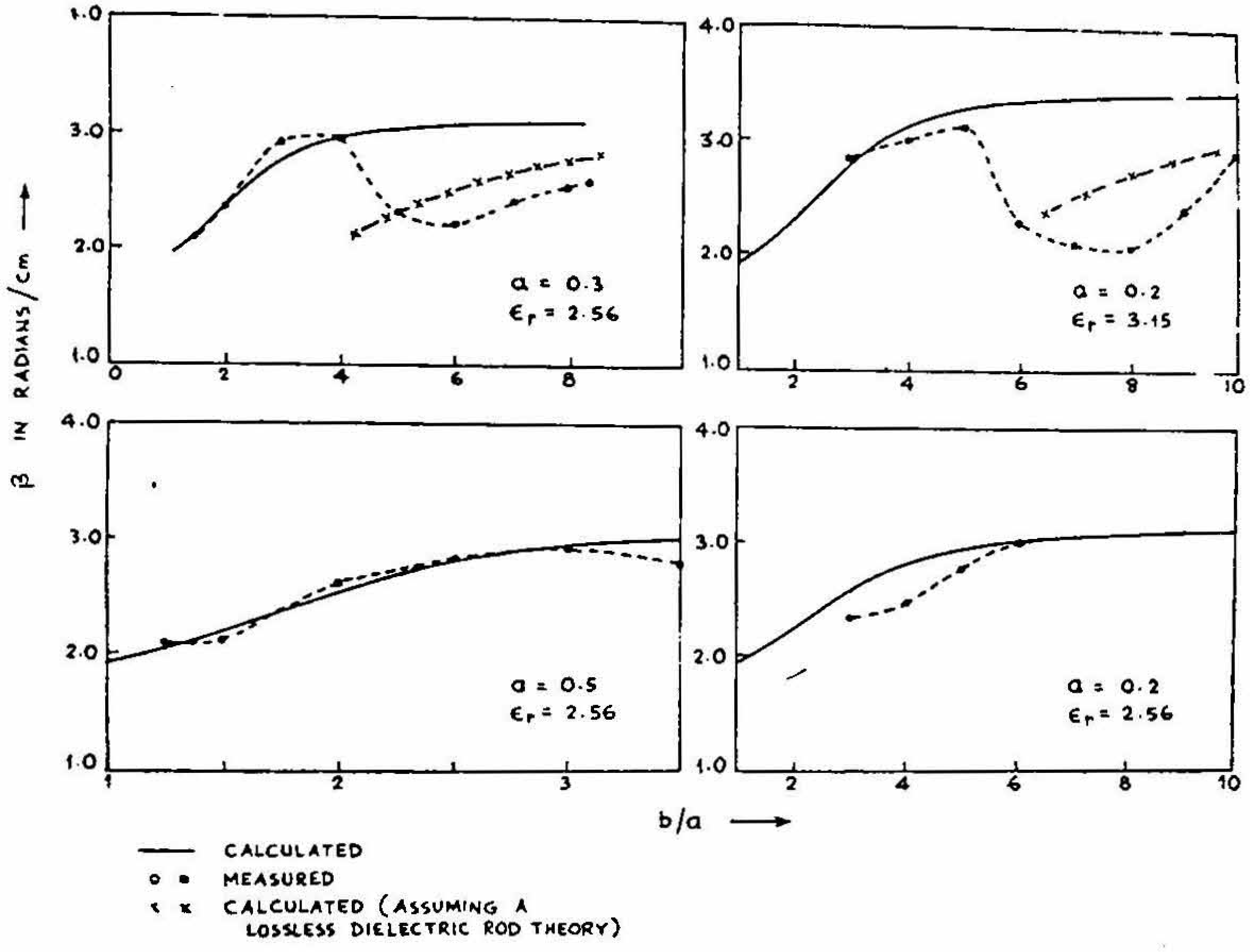

Fig. 24

12. Conclusions

The following conclusions may be drawn from the above investigations:

1. The previous work on the propagation of electromagnetic waves over a dielectric-coated conductor by different authors considered the conductor to be infinitely conducting and the dielectric coatings to be lossless and thin. It provides very little information about the propagation characteristics of electromagnetic waves over a cylindrical conductor thickly coated with a lossy dielectric material.

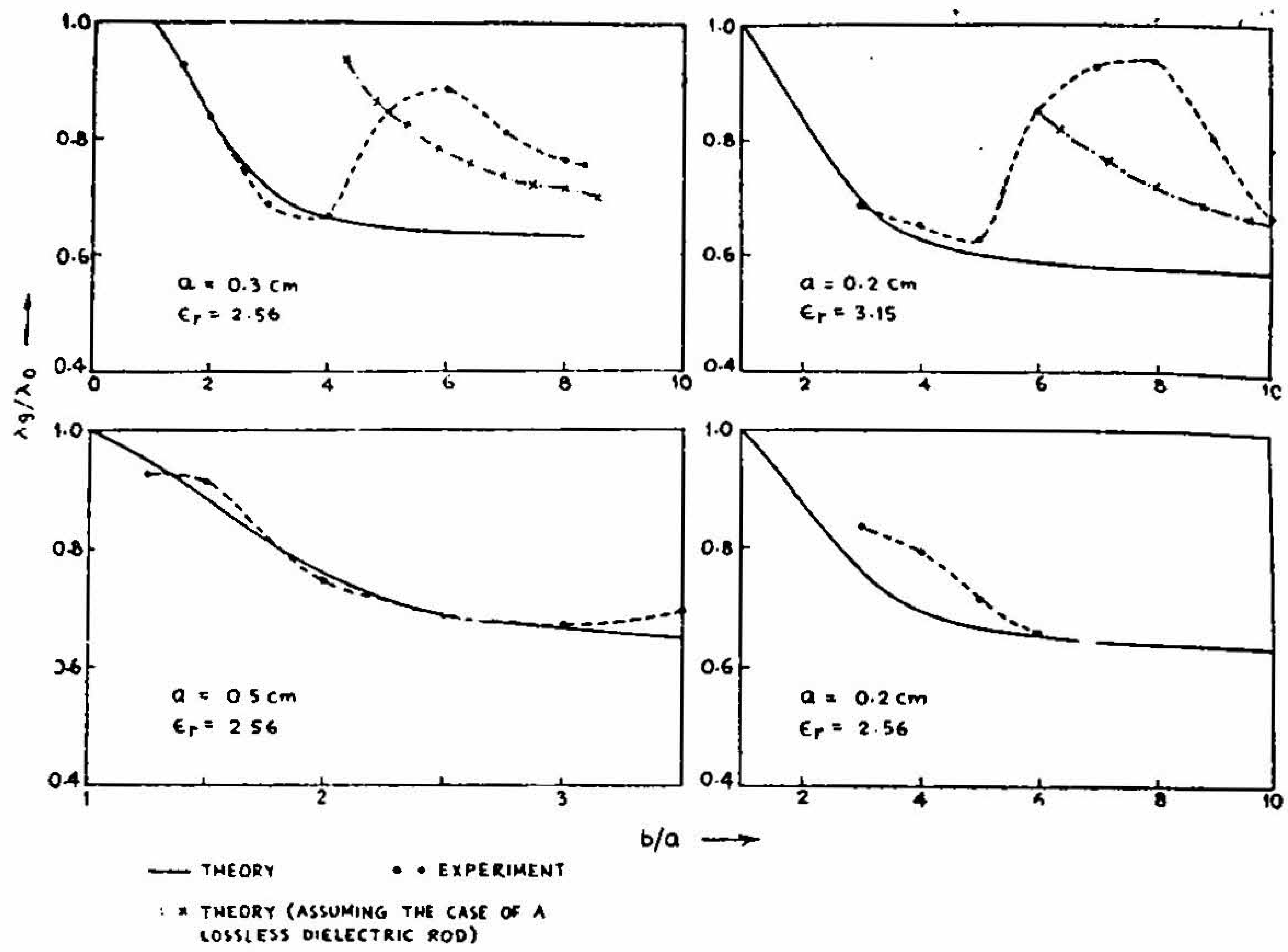

FIG. 25. Comparative study of the guide wavelength.

2. The theoretical values of the various surface wave characteristics like the guide wavelength, the phase constant and the radial field decay agree with the experiment fairly well as long as the dielectric coating is thin. This confirms the fact that a thin dielectric coated conductor is a good surface waveguide, as predicted by the earlier investigators.

3. For a thickly coated conductor, the results of the experimental investigations deviate with the corresponding theoretical results after a certain coatingthickness is exceeded. The discrepancy between the theoretical and experimental values of the phase constant β, the guide wavelength λ_g, and the radial field decay occur approximately at the same b/a ratio. This discrepancy may probably be due to the occurrence of higher order modes or of leaky waves for thick dielectric coatings, which have been neglected in the present study.

4. The theoretical results obtained for thin lossless diolectric coatings compare very well with the results of previous workers like Goubau[3-5] and Semenov[20,21].

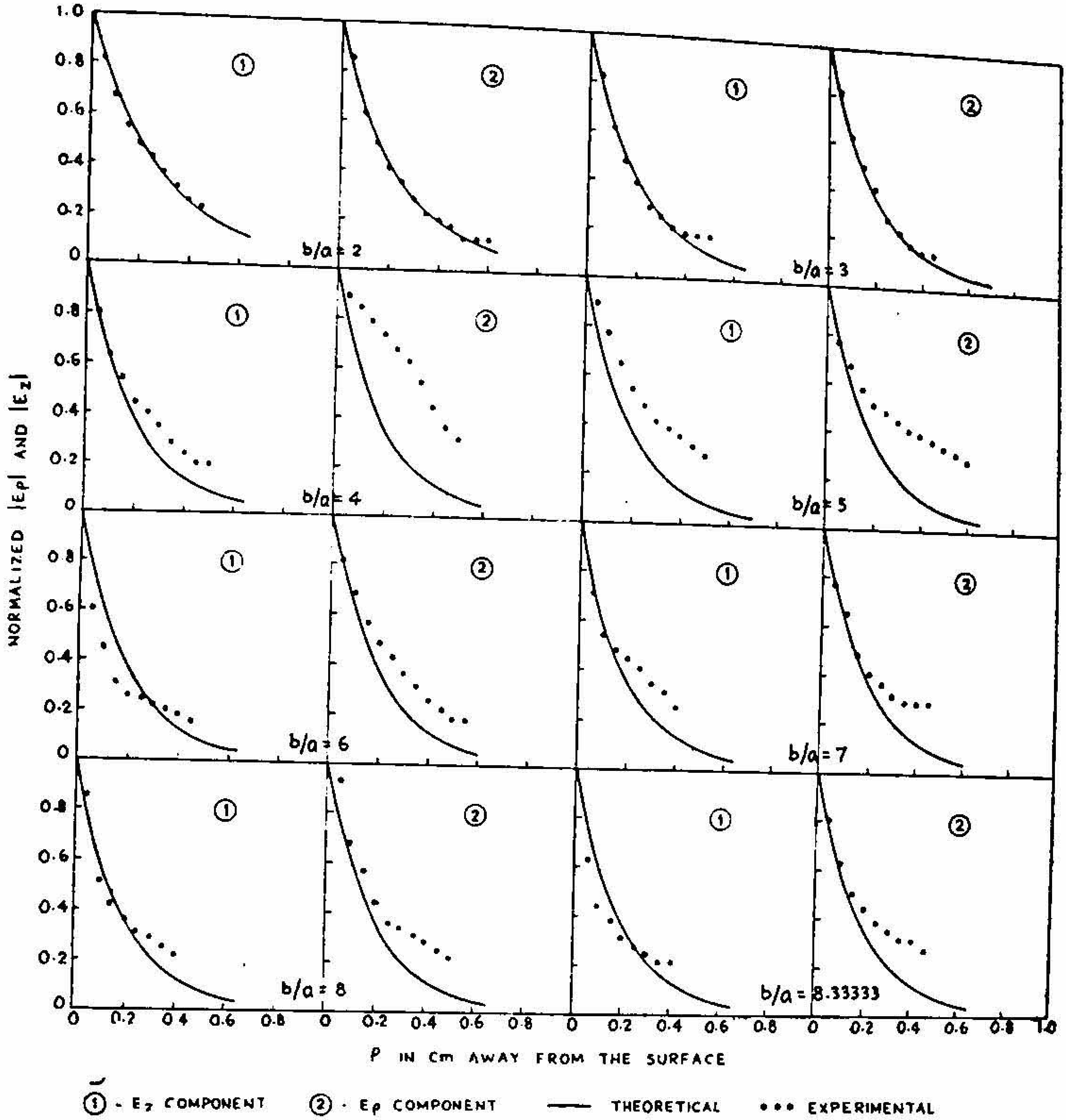

FIG. 26. Comparative study of the radial field decay (thick dielectric coatings). $a = 0{\cdot}3$, $\epsilon_r = 2{\cdot}56$.

More details of the above investigations are reported in (23).

13. ACKNOWLEDGEMENTS

The authors wish to thank Dr. S. Dhawan, Director of the Indian Institute of Science, for his encouragement for the work, and the authorities of the C.S.I.R. for the Senior Research Fellowship awarded to one of them (T. C. Rao).

14. REFERENCES

1. Harms, F. .. Electromagnetische Wellen an Einem Draht mit Isolierender Zylindrischer Hülle. *Ann. Phys.*, 1907, **23**, 44–60.

2. Goubau, G. .. Surface waves and their application to transmission lines. *Journ. Appl. Phys.*, November 1950, **21**, 1119–1128.

3. ———— .. Surface wave transmission line. *Radio Television News*, 1950, **14**, 10.

4. ———— .. Surface wave transmission line. *Radio and Electronic Engg.*, May 1950, **14** (10–11), 29–30.

5. ———— .. Single conductor surface wave transmission lines. *Proc. I.R.E.*, June 1951, **39**, 619–624.

6. Barlow, H. W. and Karbowiak, A. E. An investigation of the characteristics of cylindrical surface waves. *Proc. Inst. Elect. Engrs.*, November 1953, Paper 1462, **100** (3), 321–328.

7. ——— and Cullen, A. L... Surface waves. *Proc. Inst. Elect. Engrs.*, November 1953, Paper 1482, **100** (3), 329–341.

8. ——— and Karbowiak, A. E. An experimental investigation of axial cylindrical surface wave supported by capacitive surfaces. *Proc. I.E.E.*, May 1955, **102 B**, Paper 1786 R, 313–322.

9. Brown, J. .. The types of waves which may exist near a guiding surface. *Proc. I.E.E.*, November 1953, **100** (3), 363–364.

10. ———— .. Some theoretical results for surface wave launchers. *I.R.E., Trans.*, December 1959, AP–7, S 169– S 174, Special Supplement.

11. Wait, J. R. .. Excitation of surface waves on conducting stratified dielectric-clad and corrugated surfaces. *Jour. Res. Nat. Bureaur-Stds.*, December 1957, **59**, 365–377.

12. Cullen, A. L. .. The excitation of a plane surface wave. *Proc. I.E.E.*, August 1954, **101** (4), 225–234.

13. ———— .. A note on the excitation of surface waves. *Proc. I.E.E.*, Monograph 239 R, Publ. May 1957, September 1957, **104** (9), 472–474.

14. Zucker, F. J. .. Theory and application of surface waves. *Nuovo Cimento*, 1952, **9** (Suppl. No. 3), 450–473.

15. ———— .. The guiding and radiation of surface waves. *Proc. of the Symposium on Modern Advances in Microwave Techniques*, Polytech. Inst. of Brooklyn, November 1954, pp. 403–435.

16. Chatterjee, S. K. and Chatterjee, R. Propagation of microwave along a solid conductor embedded in three coaxial dielectrics. *Jour. Ind. Inst. Sci.*, 1956, **38 B**, 157–171 and 1957, **39 B**, 71–82.

17. ——— and Madhavan, P... Propagation of microwaves on a single wire. *Journ. Ind. Inst. Sci.*, 1955, **37 B**, 200.

18. Colin, J. F. .. Etude de la Propagation d'une onde electromagnetique par une surface metalleque reconverte d'une Couche de di-electrique, *L'onde Electrique* May 1951, **31**, 245–256.

19. Bercili, T. .. *Acta Tech. Hungar.*, 1959, **25** (3–4), 257–276.

20. Semenof, N. A. .. Wave modes in a surface wave line. *Radio Engg. and Electronic Phys.*, 1964, **9**, 989-995.

21. ———— .. Power carried by the E_{11} mode in a surface wave line. *Radio Technika (USSR)*, **22** (3), 34–42; English translation in *Telecommunications Radio Engineering* February 1967, **22** (2), Part II (U.S.A.), 94–100.

22. Kikuchi and Yamashita .. Hybrid transmission modes of Goubau line. *Jour. Inst. Elect. Commn. Engrs. Japan*, 1960, **43**, 39.

23. Chandrakaladhara Rao, T. Surface wave and radiation characteristics of a circular cylindrical dielectric-coated metal rod. *Ph.D. Thesis*, Indian Institute of Science, Bangalore-12, submitted July 1972.